Design, Synthesis and Biological Evaluation of P2-modified Proline Analogues Targeting the HtrA Serine Protease in *Chlamydia*

Jimin Hwang[a¥], Natalie Strange[b¥], Rami Mazraanib[b], Matthew J. Philips[b], Allan B. Gamble[a]*, Wilhelmina M. Huston[b*], and Joel D.A. Tyndall[a]*

[a]*School of Pharmacy, University of Otago, Dunedin, New Zealand*

[b]*School of Life Sciences, Faculty of Science, University of Technology Sydney, New South Wales, Australia*

¥ Equal contributions

*Joint Corresponding Authors: Allan B. Gamble, Wilhelmina M. Huston, Joel D.A. Tyndall

Email address: allan.gamble@otago.ac.nz, Wilhelmina.Huston@uts.edu.au, joel.tyndall@otago.ac.nz

Full postal address: [a]School of Pharmacy, University of Otago, PO Box 56, Dunedin 9054, New Zealand;

[b]School of Life Sciences, Level 4, Building 4, UTS City Campus, Cnr Harris and Thomas St Broadway NSW 2007 Australia

Highlights:

- Proline-based analogues were developed as CtHtrA protease inhibitors
- Proline-modified analogues were designed by ring expansion and substitution
- Triazole-substituted proline analogues were synthesized by azide-alkyne cycloaddition
- Compound **49** improved potency and selectivity by 8 and 22-fold, respectively over **1**
- Compound **49** exhibited potent anti-chlamydial activity in bacterial cell assays

Graphical Abstract:

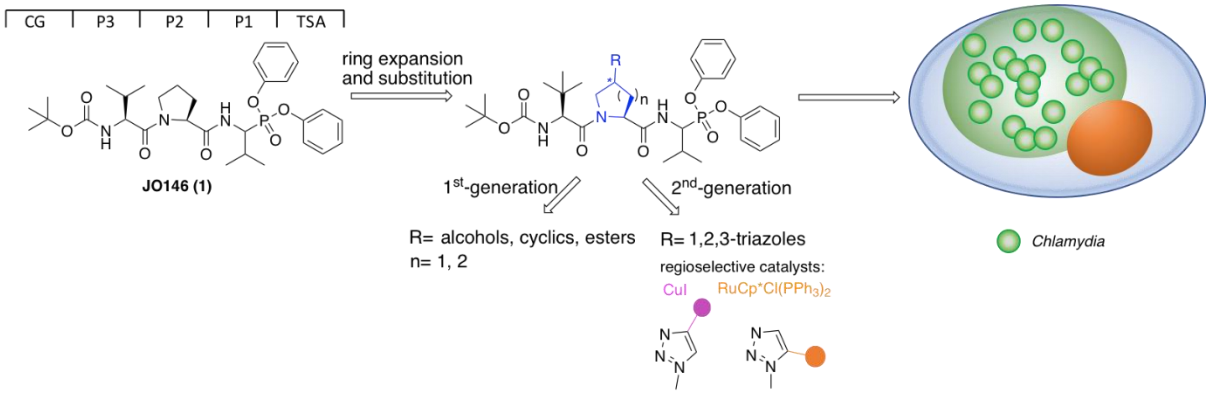

Keywords:

Chlamydia; HtrA; serine protease; inhibitor; proline analogue; triazole;

Abstract

High temperature requirement A (HtrA) serine proteases have emerged as a novel class of antibacterial target, which are crucial in protein quality control and are involved in the pathogenesis of a wide array of bacterial infections. Previously, we demonstrated that HtrA in *Chlamydia* is essential for bacterial survival, replication and virulence. Here, we report a new series of proline (P2)-modified inhibitors of *Chlamydia trachomatis* HtrA (CtHtrA) developed by proline ring expansion and Cγ-substitutions. The structure-based drug optimization process was guided by molecular modelling and *in vitro* pharmacological evaluation of inhibitory potency, selectivity and cytotoxicity. Compound **25** from the first-generation 4-substituted proline analogues increased antiCtHtrA potency and selectivity over human neutrophil elastase (HNE) by approximately 6- and 12-fold, respectively, relative to the peptidic lead compound **1**. Based on this compound, second-generation substituted proline residues containing 1,2,3-triazole moieties were synthesized by regioselective azide-alkyne click chemistry. Compound **49** demonstrated significantly improved antichlamydial activity in whole cell assays, diminishing the bacterial infectious progeny below the detection limit at the lowest dose tested. Compound **49** resulted in approximately 9- and 22-fold improvement in the inhibitory potency and selectivity relative to **1**, respectively. To date, compound **49** is the most potent HtrA inhibitor developed against *Chlamydia spp.*

1. Introduction

Chlamydia trachomatis is an intracellular Gram-negative bacterium and the leading cause of sexually transmitted infection worldwide [1]. Inappropriate or delayed treatments could lead to bacterial persistence and sequelae including pelvic inflammatory diseases, reactive arthritis, ectopic pregnancy and infertility [2, 3]. The current use of broad-spectrum azithromycin as a first-line antibiotic therapy for treating *Chlamydia* has been reported to cause extensive antibacterial resistance in commonly co-infected bacteria such as *Mycoplasma genitalium* [4, 5] and *Neisseria gonorrhoeae* [6-8], both of which have emerged as superbugs with limited treatment options. Therefore, developing narrow-spectrum antibacterial agents can reduce the spread of antibacterial resistance in clinically relevant infections.

Chlamydia pecorum is implicated as the leading cause of death in koalas (*Phascolarctos cinereus*), which are currently listed as vulnerable in Australia and predicted to become extinct by 2050 if no immediate action is taken [9-11]. Due to their fast metabolism and unique

microflora required for the digestion of *Eucalyptus* leaves, most traditional broad spectrum antibiotics used to treat humans are not appropriate in koalas [12], necessitating an urgent development of antichlamydial drugs with a narrow spectrum of action.

Rational development of antibiotics that inhibit new biological targets with a refined bacterial spectrum of action (i.e. either genus or species specific) is important to compete with the rise of antibiotic resistance and ensure continued disease prevention or treatment [13]. As traditional antibacterial targets and their new leads have become increasingly exhausted, much attention is shifting toward targeting bacterial proteases for developing novel drug candidates [14-18].

Bacterial HtrA proteins are emerging as an attractive target for drug development [14, 19]. HtrAs (also known as DegP, DegQ, DegS, MucD, PKF, YkdA and protease DO in various bacteria) [20, 21] are a serine protease ubiquitous in eukaryotic and prokaryotic cells [22]. These proteolytic and chaperone-like proteins are involved in protein quality control. Their synergistic role in removing misfolded proteins is critical under stress conditions (heat shock, oxidative, osmotic, and pH stresses) during bacterial dissemination where production of denatured proteins is accelerated [19]. HtrA proteins are also a key virulence factor in numerous bacteria, hence antivirulence strategies targeting the HtrA proteins have been investigated recently to tackle the antibiotic resistance crisis [19, 23]. Previously, we demonstrated that chemical inhibition of the *C. trachomatis* HtrA (CtHtrA), by **JO146** (**1**; **Fig. 1**) significantly altered the bacterial cell morphology, diminished inclusion vacuoles and ultimately the infectious progeny of *C. trachomatis* and *C. pecorum* [24]. Therefore, given its crucial role in the pathogenesis, replication and survival of *Chlamydia*, CtHtrA has been considered a potential drug target.

Our goal has been to develop potent and selective, covalent inhibitors of CtHtrA that provide alternative therapeutics to the current broad spectrum antichlamydial drugs for humans as well as koalas. In our previous studies, both peptidic and nonpeptidic, pyridone-based CtHtrA inhibitors were developed from site-specific modifications [25, 26] of **1**, a tripeptidic covalent lead compound (**1**; IC_{50} 12.5 μM), which was effective against *Chlamydia* strains yet inactive against *E. coli*, *Pseudomonas aeruginosa* and *Staphylococcus aureus* [26]. Compound **1** demonstrated good selectivity for CtHtrA over human HtrA homologues and serine proteases such as chymotrypsin and trypsin, however inhibited HNE at a low micromolar concentration

[24].Unnatural amino acids provide a number of advantages, including the capacity to improve target specificity, stability, and bioavailability while mimicking the physicochemical properties of natural substrates [27]. Due to its unique cyclic structure, proline is critical in biological recognition and structural motifs in a wide array of therapeutics, and has frequently been explored as a template and starting point for derivation of peptidic leads [28]. For instance, proline-mimetics as well as substituted prolines in inhibitors targeting angiotensin-converting enzyme [29] and hepatitis C NS3 protease [30] have successfully advanced into the clinic. In a continuing effort to develop more potent and selective antichlamydial drugs, herein, two generations of proline-based amino acid analogues were developed from the newer lead compound **2** [25] (with improved antiCtHtrA activity over **1**) by proline ring expansion in the conserved tripeptidic structure as well as extended substitutions at Cγ position of proline with a diverse range of functional groups (e.g. cyclics, esters, ionisable alkyls and triazoles; **Fig. 1**). Stereochemistry of Cγ-substitutions was investigated with regards to proline ring puckering and structure activity relationships (SAR) with the S2 binding pocket.

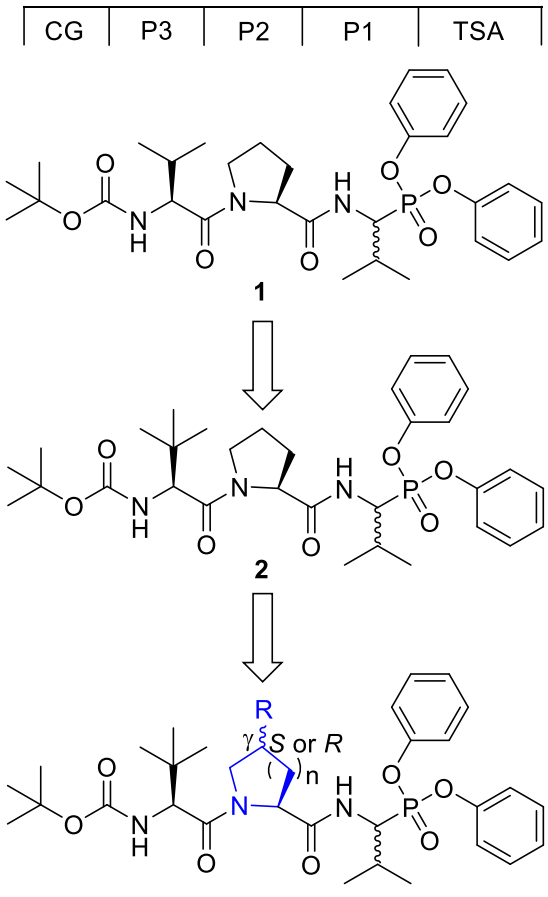

4-substituted proline analogues of **2**

Fig. 1. **JO146** (**1**) identified from high throughput screening [24] and a newer lead compound **2** obtained in previous optimization of P3 [25]. In this paper two generations of proline-based amino acid analogues of **2** are proposed and developed by proline ring expansion and Cγ-substitution. Standard nomenclature for peptide substrates in which amino acid residues are denoted as P3-P1 [31]. TSA – Transition State Analogue. CG – Capping Group.

The second-generation 4-substituted proline analogues were designed using the 1,2,3-triazole substituent at Cγ of the P2 proline residue. The triazole moiety is found in diverse bioactive compounds that act as potential new drugs to treat bacterial, fungal, viral and malarial infections [32-40]. Triazoles were synthesized by azide-alkyne cycloaddition click chemistry using ruthenium- and copper-based catalysts allowing regioselective 1,5- and 1,4-substitutions of various functional groups. A library of triazole analogues with different polar substituents were designed in an attempt to enhance the binding affinity by interacting with the S2 pocket. Docking experiments and biological assays were conducted to investigate the SAR of these novel compounds.

2. Results and Discussion

2.1. Chemistry

2.1.1. First-generation proline-based amino acid analogues

The first-generation 4-substituted proline analogues, and compound **19**, which contains a pipecolic acid in place of proline, were designed based on the lead compound structure N-Boc-Tle-Pro-Val-Phosphonate **2**, with extended P2 proline substituents including hydroxyl, ester, aromatic and carbocyclic groups (**Scheme 1** and **2**).

Lead compounds **1** and **2** were synthesized using previously reported methods [25]. In general, compounds **19-23** were synthesized by a series of solution-phase peptide coupling reactions and base-catalyzed ester hydrolysis (**Scheme 1**). Starting materials 4*S*-phenyl-L-proline (**3a**) and 4*S*-cyclohexyl-L-proline (**3b**) were esterified in the presence of a few drops of a sulfuric acid catalyst. The resulting compounds **4a** and **4b**, and commercially available *S*-methyl piperidine-2-carboxylic acid hydrochloride (**5**) and 4*S*- and 4*R*-hydroxy proline methyl esters (**6a** and **6b**, respectively) were coupled with N-Boc-Tle-OH (**7**) to produce 'N-Boc-Tle-P2-'

dipeptide intermediates (**8-12)**. Rotamerisation of compound **8** (with a pipecolic acid at P2) was confirmed by coalescence of peaks in variable temperature NMR (**Fig. S1**) and a single peak detection in analytical HPLC. The dipeptide esters were hydrolysed to give acids (**13-17**), which were then coupled to the hydrobromide salt of 1-aminoalkylphosphonate diaryl ester **18** [25, 41] to obtain the final 4-substituted proline analogues **19-23**.

Scheme 1. General Route for the Preparation of inhibitors

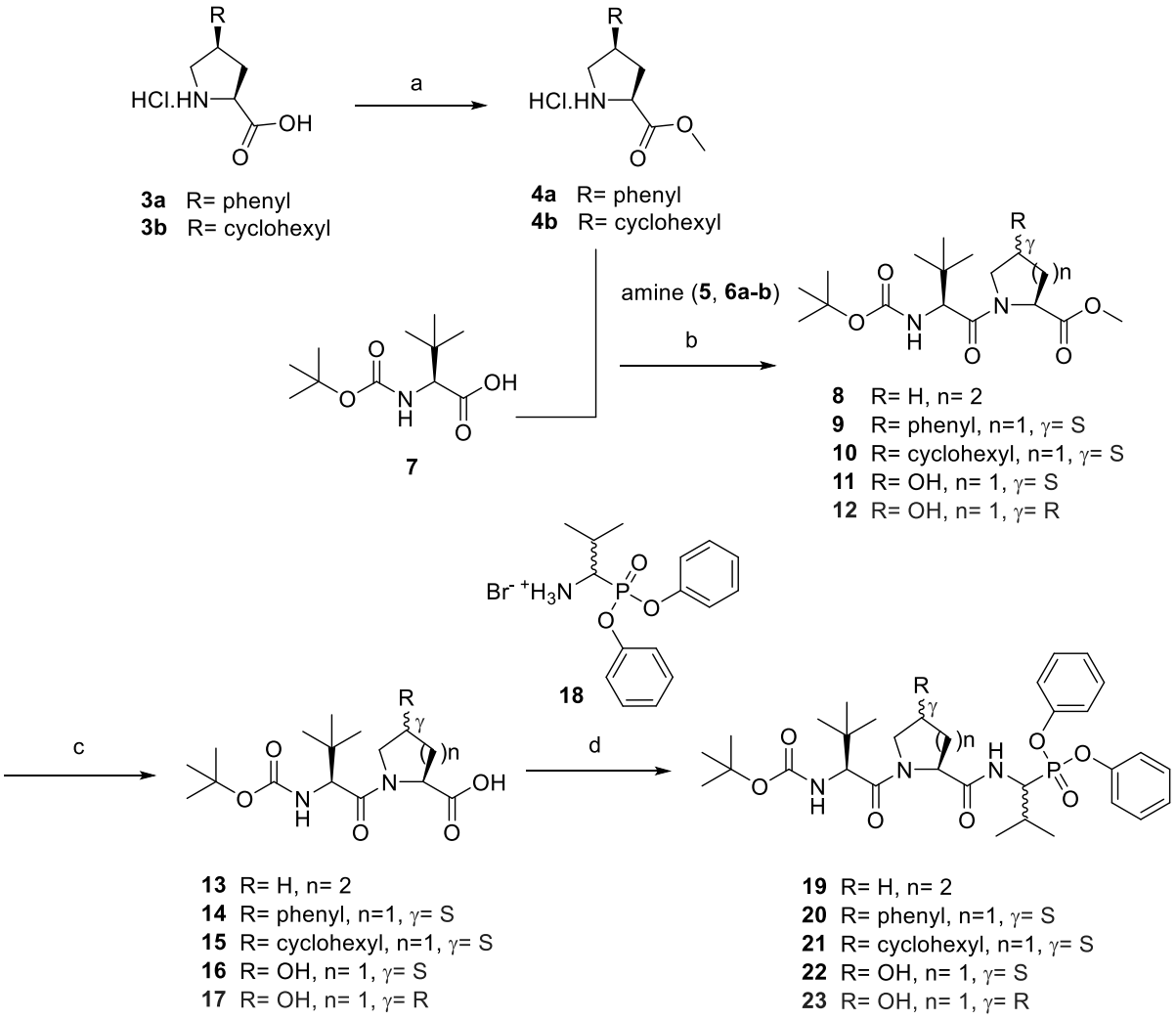

Reagents and conditions: (a) H_2SO_4, MeOH, 50 °C, overnight, 96%-quant. (b) Amine (**4a-b**, **5** and **6a-b**), HBTU, DIPEA, DMF, rt, 24 h, 26–68% (c) $LiOH.H_2O$, THF/H_2O, rt, 3 h, 58–quant. (d) **18**, HBTU, DIPEA, DMF, rt, 24 h, 47–84%.

The 4*R*-hydroxyl proline of **17** and **23**, were acylated to form an ester linkage with aliphatic chains of varying lengths and functional groups to produce the final compounds **25**, **28** and **29** (**Scheme 2**). Compound **24** was obtained by acetylating the 4*R*-hydroxyl proline in **17** with acetic anhydride in the presence of anhydrous sodium bicarbonate as a non-toxic, environmentally-friendly catalyst in replacement of a traditional organic base such as triethylamine or pyridine. Acetylation of the alcohol group in compound **23** with Fmoc-protected glycine and β-alanine was carried out by Steglich esterification with an equimolar addition of DCC and 10 mol% DMAP catalyst to yield **26** and **27**, respectively. The Fmoc-protected aminoalkyl substituents were then deprotected with 5% piperidine to yield the final compounds **28** and **29**, which were purified by semi-preparative RP-HPLC as trifluoroacetic acetate salts. Interestingly, the same reaction with compound **22** containing the inverse 4*S*-configuration of the hydroxyl proline was not as successful, giving only a negligible amount of the acetylated product detected by mass spectrometry, while the starting material remained mostly unreacted. 3D molecular modelling of an energy minimized compound **22** using Avogadro® software suggested that the 4*S*-hydroxy group faces towards the diphenyl phosphonate group, which might create steric hindrance around the hydroxyl group. Nucleophilic attack of the activated amide intermediate would thus be hindered and prevent the formation of the ester product (**Fig. S2**).

Scheme 2. General Route for the Preparation of Cγ-ester analogues 25, 28 and 29.

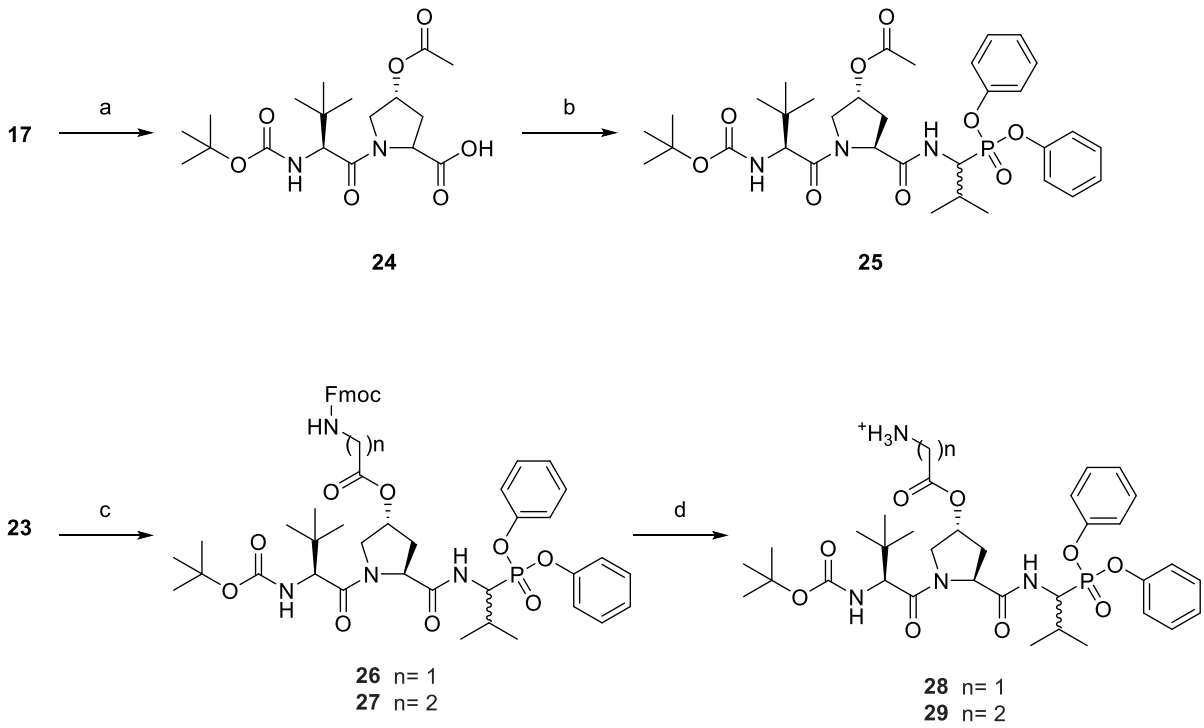

Reagents and conditions: (a) Ac_2O, $NaHCO_3$, DCM, rt, 24 h, 87% (b) **18**, HBTU, DIPEA, DMF, rt, 24 h, 49% (c) Fmoc-glycine or Fmoc-β-alanine, DCC, DMAP, DMF, 0 °C–rt, 30–50% (d) 5% piperidine, DMF, rt, 1-2 h, quant.

2.1.2. Second-generation triazole-substituted proline analogues

The second-generation 4-substituted proline analogues were synthesized to optimize **25** with enhanced antichlamydial activity. The design of derivatives of **25** was aimed at replacing the hydrolysable ester group with a more stable entity, and reducing conformational flexibility of the aliphatic chain to lower the cost of conformational entropy in binding. Rigidification of the side chain by introducing a cyclic moiety was expected to better orient the polar substituents to interact with aspartate and histidine residues surrounding the S2 pocket. Triazoles were considered a suitable scaffold that can be structurally functionalized with different substituents without generating a chiral centre as it would with an aliphatic ring. In addition, facile synthesis of triazoles by azide-alkyne click chemistry has rendered wide utility in all aspects of drug discovery ranging from lead identification to optimization [40]. Triazole moieties are also attractive because they are stable to metabolic degradation, capable of hydrogen bonding with biomolecular targets, and soluble in aqueous media [42, 43].

Firstly, the alcohol group in **11** and **12,** containing 4*S*- and 4*R*-hydroxyl proline, respectively, was mesylated prior to the S_N2-mediated Mitsunobu reaction with sodium azide, which caused the secondary alcohols to undergo inversion of their stereogenic centres [44]. The resulting azides **30** and **31** were then clicked to a range of alkynes with polar -OH or -NH substituents, such as propiolamide, 2-butyne-1,4-diol, 2-methyl-3-butyn-2-ol and propargyl alcohol, to obtain **32-41** (**Scheme 3**). The resulting esters were then hydrolysed and submitted for peptide coupling with **18** to afford final compounds **42-50**.

Scheme 3. General Route for triazole analogues

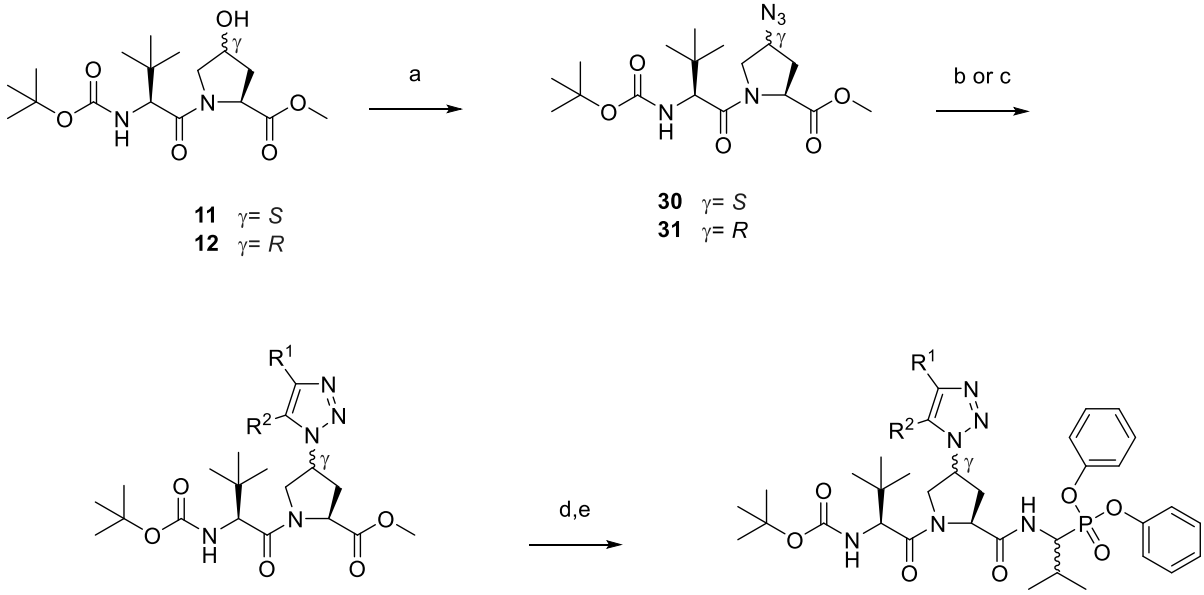

32 R^1= OH, R^2= OH, γ= *R*
33 R^1= OH, R^2= OH, γ= *S*
34 R^1= $C(CH_3)_2OH$, R^2= H, γ= *R*
35 R^1= CH_2OH, R^2= H, γ= *R*
36 R^1= CH_2OH, R^2= H, γ= *S*
37 R^1= $CONH_2$, R^2= H, γ= *R*
38 R^1= H, R^2= $C(CH_3)_2OH$, γ= *R*
39 R^1= H, R^2= $C(CH_3)_2OH$, γ= *S*
40 R^1= H, R^2= $CONH_2$, γ= *R*
41 R^1= H, R^2= CH_2OH, γ= *S*

42 R^1= OH, R^2= OH, γ= *R*
43 R^1= OH, R^2= OH, γ= *S*
44 R^1= $C(CH_3)_2OH$, R^2= H, γ= *R*
45 R^1= CH_2OH, R^2= H, γ= *R*
46 R^1= CH_2OH, R^2= H, γ= *S*
47 R^1= $CONH_2$, R^2= H, γ= *R*
48 R^1= H, R^2= $C(CH_3)_2OH$, γ= *R*
49 R^1= H, R^2= $C(CH_3)_2OH$, γ= *S*
50 R^1= H, R^2= $CONH_2$, γ= *S*

Reagents and conditions: (a) triethylamine, MsCl, NaN_3, DCM, 0 °C–rt, overnight, 61–64% (b) alkyne, DIPEA, CuI, THF or DMF, rt, overnight, 59–96%, (c) alkyne, $RuCp^*Cl(PPh_3)_2$, dioxane, 60 °C, overnight, 35–85%, (d) LiOH, H_2O, H_2O/THF, 3 h, quant. (e) **18**, HBTU, DIPEA, DMF, rt, 24 h, 30–85%.

Complementary pairings between CuAAC and RuAAC with two alkyne substrates, 2-methyl-3-butyn-2-ol and propiolamide, were conducted to investigate their optimal substitution position on the triazole for interacting with residues in the S2 pocket. Also, the pairs (**34** with **38**, **36** with **41**, and **37** with **40**) were used for comparison and validation for the regioselectivity of the two metal catalysts by NMR (**Table S1**). The differences in the proton chemical shifts of H_A and H_B indicated that the surrounding electronics of H_A and H_B differed slightly from each other (see **Table S1**); and the absence of the proton peak corresponding to the other possible regioisomer in these compounds verified clean regioselectivity of the CuI and RuCp*Cl$(PPh_3)_2$-catalysed click reaction with the selected alkyne reagents (*supplementary information*).

A 2D HMBC NMR experiment was also used to differentiate the 1,4-substitution of **36** from the 1,5-substituted compound **41** (**Fig. 2**). With 1,4-substitution, the coupling between H_B and Cγ of proline, and between C5' of triazole and H_c were observed (**Fig. S3**). On the other hand, none of these couplings were present in the complementary 1,5-substituted compound **41** (**Fig. S4**).

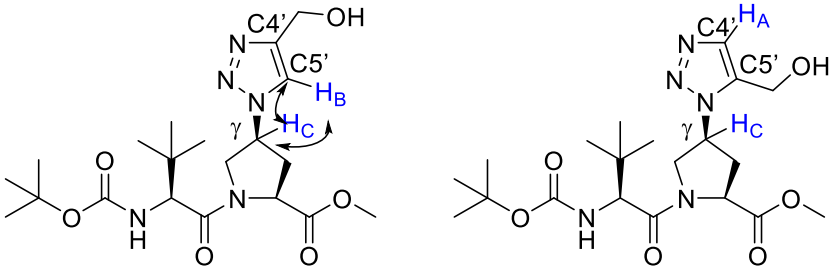

Fig. 2. 1,4-Substituted compound **36** (left) was differentiated from 1,5-substituted compound **41** (right) by a 2D HMBC NMR experiment.

2.2. Enzyme assays

Protease inhibition assays were conducted for inhibitory activity and off-target characterization of the final compounds. IC_{50} values were measured to assess the inhibitory activities of compounds against CtHtrA (**Table S2** and **Table S3**) [45, 46] and HNE (**Table S4**) [26]. The IC_{50} values varied in different batches of the CtHtrA assays (**Table S2** and **Table S3**), hence relative potency and selectivity of compounds were determined (compared to **1)** for evaluating their biological activities [25, 26]. Observed inconsistencies of IC_{50} values between different

batches are speculated to be caused by the requirement of the HtrA protease to undergo activation via peptide binding to the PDZ domain for optimal enzymatic activity. Recombinant protein may be co-purified with short activating peptides from the expression host, which can vary between batches and escape detection by SDS-PAGE analysis [47]. In addition, structural rearrangement to higher degree oligomers (e.g. from the inactive 6-mer to 12- or 24-mer via activation) is linked with both proteolytic and chaperone capabilities [45].

2.2.1. First-generation proline-based amino acid analogues

Ring expansion of proline to a six-membered piperidine ring in compound **19** resulted in about 4 to 5-fold decrease in the inhibitory activity against CtHtrA compared to the lead compounds **1** and **2** (**Table 1**). Cγ-substitution of bulky, non-polar cyclic rings in proline as in compounds **20** and **21** was unfavourable, decreasing the inhibitory potency by approximately 3- and 7-fold, respectively, relative to **1**. Compound **21** displayed a large 95% confidence interval of the IC_{50} ranging from 89 to 523 μM and a poor R^2 (fitness of the curve), underlining a poor inhibitory mechanism against CtHtrA (**Table S2**). 4*R*-Hydroxyproline with *trans* stereochemistry (**23**), oriented towards the S2 pocket, was equipotent to **2** (lead compound) against CtHtrA. However, altering the configuration to the 4*S* or *cis* form (**22**) led to reduced antiCtHtrA activity.

Table 1. Inhibitory activities of inhibitors against CtHtrA and HNE.

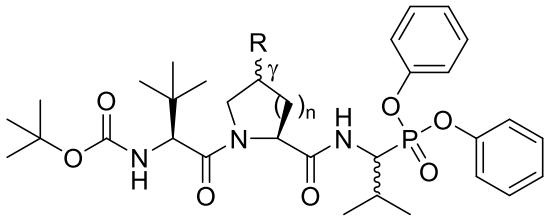

Cpd	n	R	γ	IC_{50} ± SEM (μM; n = 3)		Relative selectivity[c]
				CtHtrA (relative inhibition against to 1[a])	HNE (relative inhibition against to 1[b])	
1	1	H	-	21.86 ± 0.43 (1.00)	1.15 ± 0.06 (1.00)	1.00
2	1	H	-	15.86 ± 0.48 (1.38)	3.02 ± 0.10 (0.38)	3.62
19	2	H	-	81.84 ± 8.58 (0.27)	4.45 ± 0.38 (0.26)	1.04
20	1	phenyl	*S*	59.50 ± 3.34 (0.37)	1.39 ± 0.14 (0.83)	0.51
21	1	cyclohexyl	*S*	163.2 ± 7.75 (0.13)	3.84 ± 0.16 (0.30)	0.45
22	1	OH	*S*	48.66 ± 0.68 (0.45)	NA	NA
23	1	OH	*R*	14.21 ± 7.28 (1.54)	2.13 ± 0.10 (0.54)	2.85
25	1	OAc	*R*	3.86 ± 0.16 (5.66)	2.36 ± 0.06 (0.49)	11.6
28	1	$OCOCHNH_3^+$	*R*	13.93 ± 0.25 (1.57)	2.69 ± 0.04 (0.43)	3.67
29	1	$OCO(CH_2)_2NH_3^+$	*R*	15.26 ± 1.15 (1.43)	1.21 ± 0.05 (0.95)	1.50

NA- Not Assessed

[a]Relative inhibition against CtHtrA is the ratio of $IC_{50\ CtHtrA}$(**1**) to $IC_{50\ CtHtrA}$ (compound).

[b]Relative inhibition against HNE is the ratio of $IC_{50\ HNE}$ (**1**) to $IC_{50\ HNE}$ (compound).

[c]Relative selectivity is the ratio of the relative potency against CtHtrA to relative potency against HNE compared to that of **1**.

The most potent antiCtHtrA analogue from the first-generation inhibitors was **25** with an acetyl group substituent. Compound **25** increased inhibitory potency by ~5.5- and 4-fold relative to **1** and **2**, respectively, while increasing the selectivity towards CtHtrA over HNE by about 12-fold relative to **1**. Aliphatic esters with primary amino functional groups (**28** and **29**) did not adversely affect the IC_{50} values relative to lead compound **2.** This indicated that the cationic amino groups were ineffective in increasing the binding affinity towards the S2 subpocket containing aspartate residues, perhaps due to the high flexibility of the linear chains that increase the entropy term of Gibbs free energy of binding. These results together suggested that rigidification of the extended aliphatic groups may provide a better avenue to optimize the proline residue.

2.2.2. Second-generation triazole-substituted proline analogues

Five compounds (**43**, **44**, **45**, **48**, **49**) from the second-generation 4-substituted proline analogues were tested for their inhibitory activity against CtHtrA and SAR analysis based on their antichlamydial potency from whole cell assays discussed below.

All triazole compounds tested in this assay showed superior CtHtrA inhibition to **1** and **2**. Compound **43** increased the inhibitory activity against CtHtrA and selectivity over HNE by more than 11-fold and 13-fold, respectively, relative to **1**. Compound **49** also markedly increased the antiCtHtrA potency by approximately 9-fold compared to **1**. In addition, **49** resulted in a slight reduction in the inhibitory activity against HNE, leading to more than 22-fold improvement in the relative selectivity over HNE. The potency and selectivity profile of **49** was superior to compound **48** with a matching triazole moiety but in *R*-configuration at the Cγ of the proline. Compounds **44** and **45**, both of which consist of a hydroxyl group in the triazole substituent in the C4' position, showed similar improvement in the inhibition of CtHtrA by 3.7 and 3.3-fold, respectively. Yet, the bulkier *tert*-butanol substituent in **44** (in comparison to an ethanol substituent in **45**) showed greater selectivity over HNE with a 10-fold improvement relative to **1**. Given the negligible difference in the IC_{50} values between **44** and **48** against CtHtrA (**Table 2**), the position of the *tert*-butanol substitution in the triazole moiety had little effect in the CtHtrA inhibition when the triazoyl group was in an *R*-configuration at Cγ.

Table 2. Inhibitory activities of triazole analogues against CtHtrA and HNE.

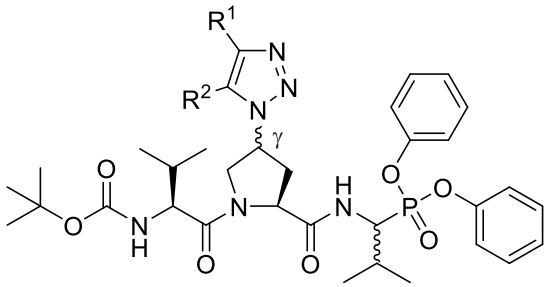

Cpd	R1	R2	γ	IC$_{50}$ ± SEM (μM; n = 3)		Relative selectivity[c]
				CtHtrA (relative inhibition against to 1[a])	HNE (relative inhibition against to 1[b])	
1	-	-	-	266.5 ± 44.3 (1.00)	1.15 ± 0.06 (1.00)	1.00
42	OH	OH	*R*	NA	2.27 ± 0.14 (0.51)	NA
43	OH	OH	*S*	23.01 ± 8.48 (11.58)	1.32 ± 0.23 (0.87)	13.3
44	$C(CH_3)_2OH$	H	*R*	71.63 ± 2.28 (3.72)	3.08 ± 0.18 (0.37)	10.1
45	CH_2OH	H	*R*	79.68 ± 5.81 (3.34)	1.06 ± 0.08 (1.08)	3.09
46	CH_2OH	H	*S*	NA	1.37 ± 0.04 (0.11)	NA
47	$CONH_2$	H	*R*	NA	2.88 ± 0.24 (0.40)	NA
48	H	$C(CH_3)_2OH$	*R*	95.72 ± 0.54 (2.78)	1.79 ± 0.02 (0.64)	4.34
49	H	$C(CH_3)_2OH$	*S*	30.27 ± 5.50 (8.80)	2.98 ± 0.10 (0.39)	22.6
50	H	$CONH_2$	*S*	NA	1.61 ± 0.05 (0.71)	NA

NA- Not Assessed

[a]Relative inhibition against CtHtrA is the ratio of $IC_{50\ CtHtrA}$(**1**) to $IC_{50\ CtHtrA}$ (compound).

[b]Relative inhibition against HNE is the ratio of $IC_{50\ HNE}$ (**1**) to $IC_{50\ HNE}$ (compound)

[c]Relative selectivity is the ratio of the relative potency against CtHtrA to relative potency against HNE compared to that of **1**.

2.3. Antibacterial activity and cytotoxicity assessments in cell-based assays

Cellular antibacterial activities of the proline-based amino acid analogues against *C. trachomatis* (**Table S5** and **Table S6**) and *C. pecorum* (**Table S7** and **Table S8**) were measured by their ability to reduce the number of inclusion-forming units (IFU/mL) [24, 26, 48]. The levels of cytotoxicity of the final compounds against HEp-2 cells were assessed by MTS and LDH assays [26], which represent cell viability and integrity, respectively.

2.3.1. First-generation proline-based amino acid analogues

All analogues from the first-generation inhibitors deterred Chlamydial growth significantly higher than DMSO control and in a dose-dependent manner (**Fig. 3**). To our surprise, despite showing weak inhibition of CtHtrA, **21** was significantly more effective in reducing the chlamydial inclusion forming units, causing an approximate 2.0-log reduction at 25 µM compared to lead compound **2**. At 50 µM, **21** diminished the bacterial titre below the detection threshold (10^4 IFU/mL). Similarly, in the *C. pecorum* assays, **21** was the most potent, eradicating the bacteria even at 25 µM (**Fig. 3**). However, this unexpectedly high antichlamydial activity of **21** was found to be non-specific cytotoxic effects as indicated by MTS and LDH cytotoxicity assays against HEp-2 cells (**Fig. 4**). Compound **21** significantly reduced the viability of HEp-2 cells, resulting in only 10 to 20% of cell viability compared to the DMSO control in the MTS assay. Compound **21** also led to the significant loss of cell integrity indicated by the 80% cytosolic LDH release, causing excessive cytotoxicity on HEp-2 cells. Therefore, its antichlamydial effect is caused by a generic cell killing, most likely to be due to poor aqueous solubility and drug aggregation in the cell media.

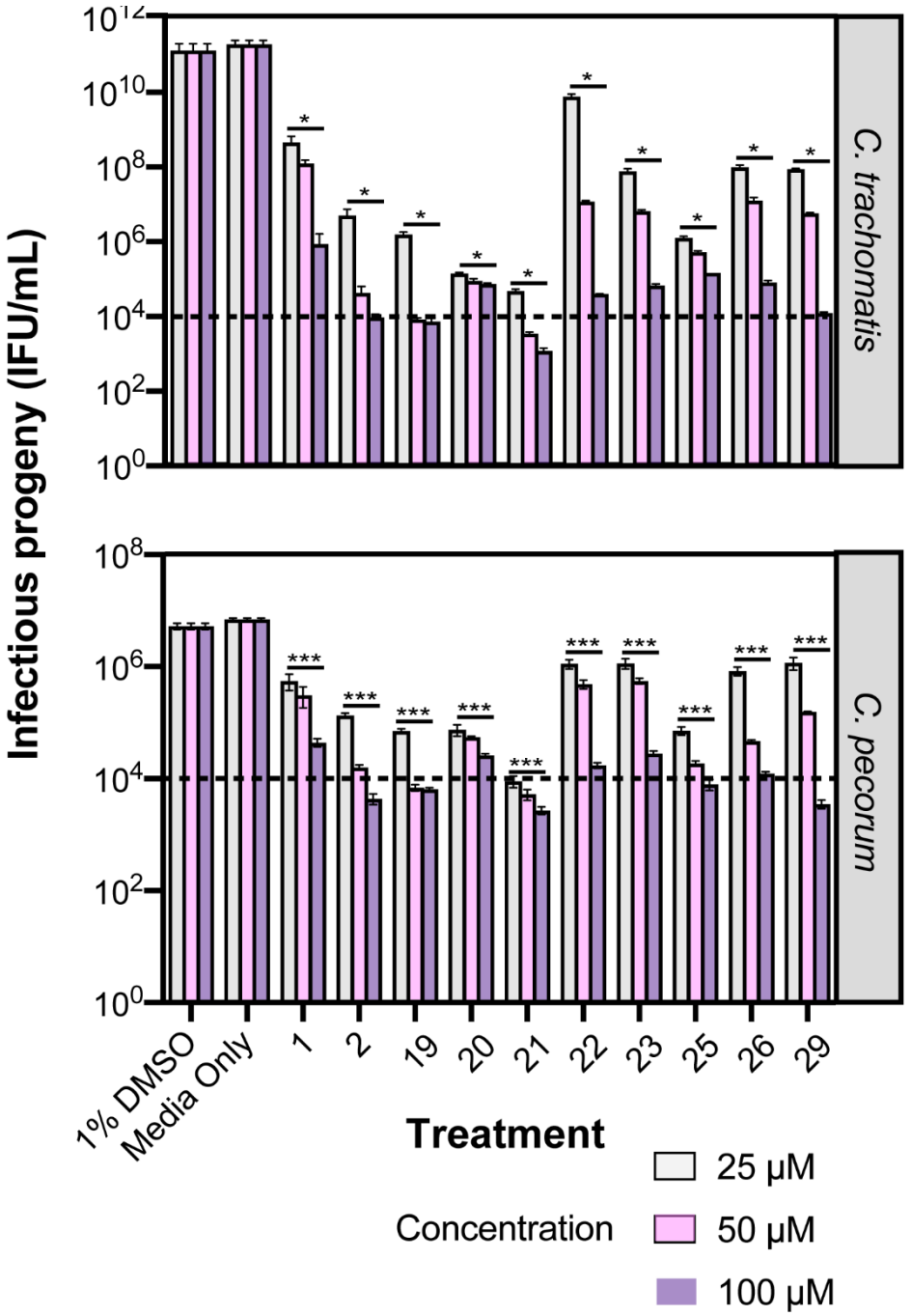

Fig. 3. Cell-based antibacterial inhibition of *Chlamydia trachomatis* and *C. pecorum* growth by the lead compounds (**1** and **2)** and first-generation 4-substituted proline analogues (**20-23**, **25**, **28** and **29**) and **19** at 25, 50 and 100 µM. Dashed line indicates the limit of detection for live chlamydial cells. Error bars represents the SEM (n = 3). Raw values of the IFU counts are reported in **Table S5** and **S7**. **p*-value <0.05 and ****p*-value <0.0001 compared to DMSO control as measured by two-way ANOVA.

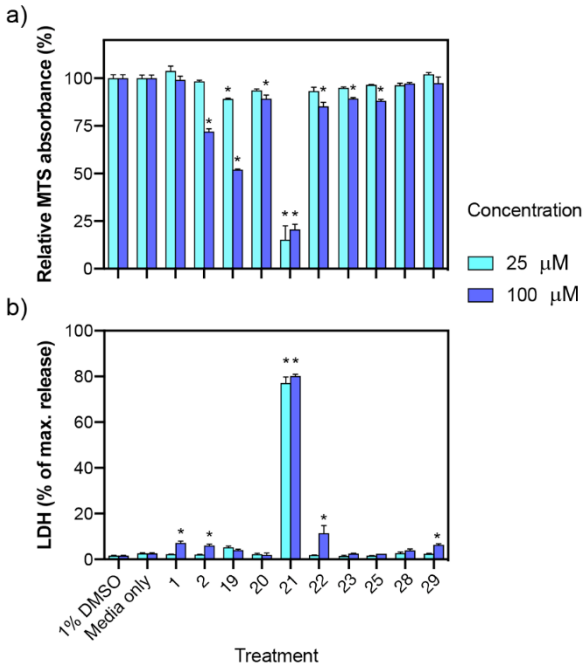

Fig. 4. (a) Viability and integrity of HEp-2 cells treated by the first-generation 4-substituted proline analogues (**20**, **21**, **22**, **23**, **25**, **28**, **29**) and **19**. (b) The percentage of extracellular LDH detected compared to maximum release controls. *Significantly different (*p*-value <0.05) from DMSO controls as measured by two-way ANOVA. Error bars represent the SEM (n = 3).

Excluding **21** for its non-selective cytotoxic effects, compound **20** showed the strongest inhibitory effect against *C. trachomatis* at 25 µM (reducing the infectious progeny by $10^{3.6}$- and $10^{1.6}$-fold greater than lead compounds **1** and **2**, respectively), closely followed by compounds **25** and **19** ($10^{2.6}$-fold and $10^{2.4}$-fold reduction in IFU/mL, respectively, compared to **1**; **Fig. 3**). In *C. pecorum* assays, **19**, **20** and **25** were equipotent antichlamydial compounds at 25 µM; yet **19** and **25** were better than **20** at higher doses, reducing the bacterial titre close to or below the limit of detection (**Fig. 3**). All first-generation inhibitors (except **21** as discussed above) resulted in less than 30% MTS reduction relative to the DMSO control at 25 µM, indicating their lack of cytotoxicity at this dose. Compound **19**, however, significantly decreased the relative cell viability to 50% in the MTS assay at 100 µM, while the level of LDH leakage was minimal relative to the control. This indicated that **19** reduced the cell proliferation and metabolic rate at a higher dose without causing cell lysis. The minimal level of extracellular LDH release by the first-generation 4-substituted proline analogues (excluding **21**) at both 25 and 100 µM concentrations showed that these analogues were not cytotoxic to HEp-2 cells (**Fig. 4**).

Despite their similar antiCtHtrA activities, the decrease in the antichlamydial potency of **28** and **29** in the cell assays relative to lead compound **2** could be attributed to the reduced ability of the cationic compounds to cross the HEp-2 host cell membrane. Although cationic peptides are known to have antibacterial effects by destabilizing the negatively charged bacterial membranes [49-51], the ionization of the **28** and **29** is likely to hinder penetration across the host cell membrane barriers.

Overall, within the first-generation 4-substituted proline analogues, compound **25** was considered for further optimization for its strong CtHtrA inhibition, antichlamydial activities and lack of cytotoxicity in HEp-2 cells. Therefore, its acetyl group was substituted with the 1,2,3-triazole template to generate second-generation 4-substituted proline analogues to further improve the antichlamydial potency relative to the lead compound **2**.

2.3.2. Second-generation triazole-substituted proline analogues

The second-generation analogues did not affect the viability of HEp-2 cells as indicated by the MTS cytotoxicity assay (**Fig. S5**). In comparison to **2**, compounds **45, 48, 49, 50** from the second-generation 4-substituted proline analogues showed superior antibacterial potency against *C. trachomatis* at all three tested doses (**Fig. 5**). The three most potent analogues **48**, **49** and **50** against *C. trachomatis* commonly possessed sterically hindered acetamide and *tert*-butanol group at the triazole C5' position. Of all second-generation compounds, **49** performed exceedingly better as it reduced the bacterial titre of *C. trachomatis* well below the limit of detection (3.4-, 2.4- and 3.2-log lower IFU/mL counts at 25, 50 and 100 µM than **2**). Compounds **45**, **48**, **49**, **50** were also more effective in reducing the bacterial titre of *C. pecorum*, resulting in approximately 1.1-, 1.0-, 2.3- and 2.6-log decrease in IFU/mL at 25 µM, respectively, compared to **2**. In *C. pecorum* assays, **49** and **50** were equally lethal to the bacteria at all three doses.

Despite the strong inhibitory activity of **43** in the enzyme assays, C4'- and C5'-dihydroxy triazole analogues **42** and **43** both demonstrated the least antichlamydial activity among the second-generation analogues. Together with **42** and **43**, compound **46**, which contained an ethanol group substituted at C4' of the triazole ring, lacked antibacterial activity against *C. pecorum* compared to the media controls. Interestingly, in contrast to compounds **22** and **23**

from the first-generation 4-substituted proline analogues, there was no correlation between the stereochemistry at the Cγ of proline and the antichlamydial activities. Overall, analogues with C5'-substituted triazoles **48-50** generally showed stronger antichlamydial activities than those with C4'-substituted triazoles **44-47**. Analogues **44-47** were more effective in reducing the bacterial load than those with C4'- and C5'- disubstituted triazoles **42** and **43,** the exception being analogue **46**, which was also ineffective in reducing infectious progeny.

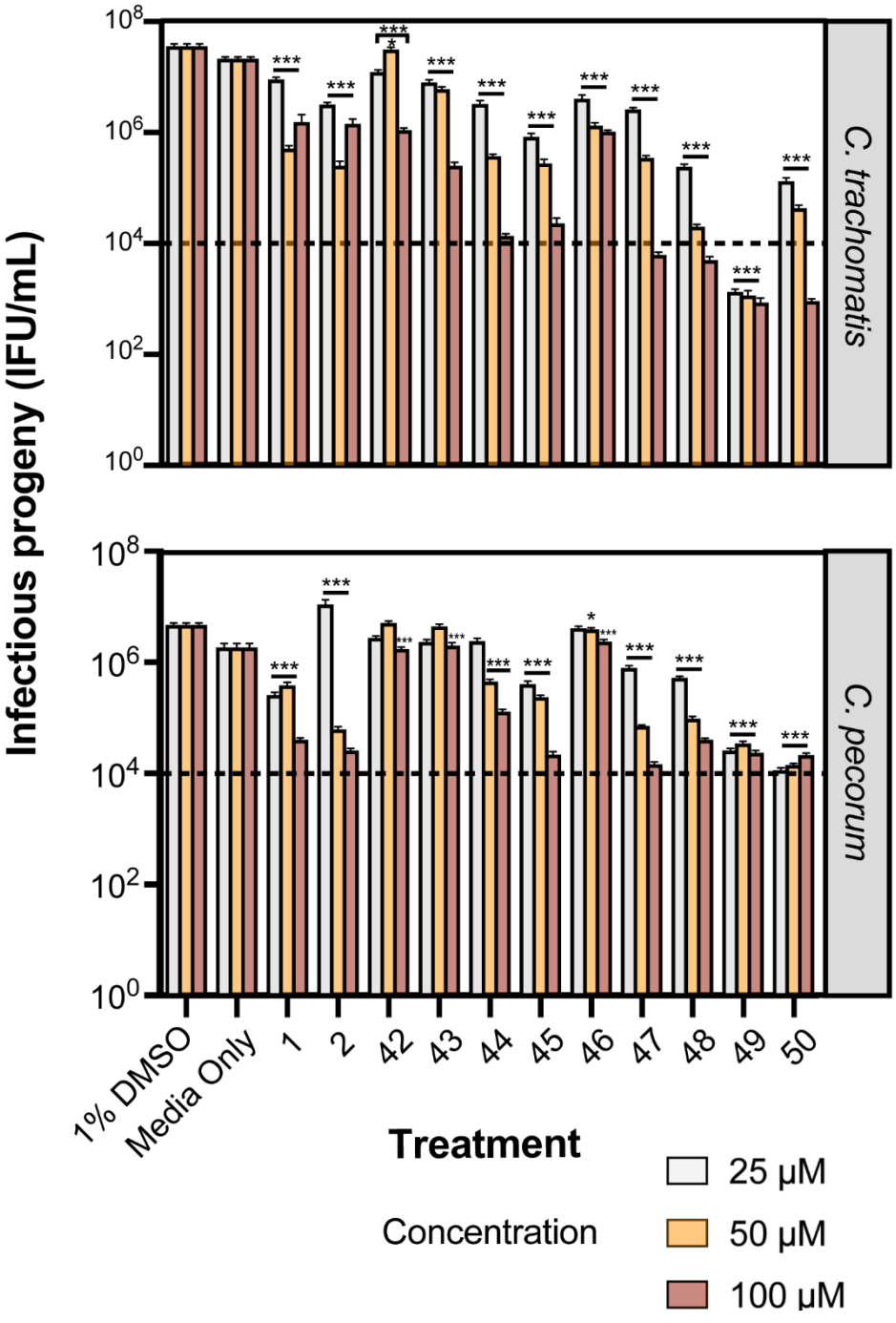

Fig. 5. Cell-based testing of inhibition of *C. trachomatis* and *C. pecorum* growth by lead compounds **1** and **2** and second-generation triazole-based analogues **42**-**50** at 25, 50 and 100 μM. Dashed lines indicate the limit of detection for live chlamydial cells. Raw values of the IFU counts are reported in **Table S6** and **S8**. Error bar represents the SEM (n = 3). **p*-value <0.05 and ****p*-value <0.0001 compared to DMSO control as measured by two-way ANOVA.

2.4. Molecular Modelling

2.4.1. Homology modelling of CtHtrA

To date, there is no X-ray crystal structure of chlamydial HtrA, and only a few structures of DegP homologues are available, including *Escherichia coli*, *Helicobactor pylori* [23] and *Mycobacterium tuberculosis* [52]. A new CtHtrA homology model was generated based on the crystal structure of *E. coli* HtrA (DegP; PDB code: 3MH6 [53]) complexed with a generic serine protease inhibitor diisopropyl phosphonate. The DegP crystal structure was selected as a model template given its relatively high percentage identity and similarity (57/77% of identity/similarity calculated by Basic Local Alignment Search Tool) compared to those of other bacteria [14]. In comparison to the formerly constructed CtHtrA homology model by Gloeckl, *et al.* (2012) [54], the new CtHtrA model was topologically identical except the orientation of the imidazole ring of His178 in L3 loop (**Fig. S6**), which was facing away from the active site instead of towards it. Given the flexibility of L3 loop, as reflected by its known rearrangement mechanism upon the protease activate cascade [55], slight variability in the positioning of residues in this loop was not unexpected.

2.4.2. Docking studies

Our design of proline-based analogues was based on the information obtained from the homology models of CtHtrA. The homology model of CtHtrA comprises a deep S2 subpocket containing ionisable non-catalytic His178 and Asp231 residues as well as the catalytic His143 and Asp173 residues within 5.0 Å of the docked position of JO146 at the active site and were considered potential targets for hydrogen-bond or electrostatic interactions with the extended polar substituents from Cγ of the proline residue.

The first- and second-generation analogues were covalently docked into CtHtrA homology model and were compared to **1**. Stereoelectronic effects of 4-substituted prolines result in a preference in the Cγ−Cδ bond for a *gauche* relationship between the amide and 4-positioned electron-withdrawing groups (EWGs; e.g., –OH, –F, azido, triazolyl) [28]. Therefore, in a (*4-trans*)-EWG substitution, *exo* puckering is preferred, whereas *endo* puckering is favoured in a (*4-cis*)-EWG substitution. Based on this, compounds with either the 4*R*-hydroxyl or acyl Cγ substituents (**23**, **25**, **28** and **29**) were docked in with an *exo* conformation. The proline puckering remained *exo* in all docked poses of these compounds even though the experiment was conducted in the "flexible ring" setting to allow freedom of the puckering mode by any external interactive forces of the protease.

Given that neither *S* or *R* configuration of the 4-hydroxyl proline was involved in hydrogen bonding at the active site, the 3.4−fold improvement in the IC_{50} for **23** (14.21 μM) compared to **22** (48.66 μM) could be due to the enhanced stabilization of the *trans* amide bond with the 4*R*-hydroxy-induced *exo* puckering of the proline ring [56, 57]. In fact, compounds with electron-withdrawing 4*R*-substituents (**23**, **25**, **28**, **29**) exhibited stronger inhibitory activities against CtHtrA than **2** and **1** lead compounds (**Table 1**).

In the first-generation of analogues, **25** showed the most promising IC_{50} (approximately 4- and 6-fold improvement relative to **2** and **1**, respectively; **Table 1**). The docking position of **25** against the homology model of CtHtrA suggested that the hydrophobic interactions (with an average 4.0 Å distance) between the acetyl-CH_3 group on **25** and the hydrophobic residues Leu227, Phe235 and Thr263 would enable a strong additive van der Waals interaction, thereby increase the inhibitory activity against CtHtrA (**Fig. 6a**).

The 4*R*-substituted terminal amine groups in the docked poses of **28** and **29** were in proximity to Asp173 (2.9 Å) and Asp231 (3.3 Å) at the S2 pocket, respectively, potentially forming strong electrostatic interactions (**Fig. 6b**). However, given the marginal improvement in the IC_{50} of **28** and **29** compared to **2**, such potential interactions were not translated to improved biological activities perhaps due to the highly flexible alkyl chains which could result in higher entropy loss in binding at the expected orientations. Therefore, structural rigidification of these polar substituents into a triazole-based template was expected to reduce the entropic penalty and improve binding affinity.

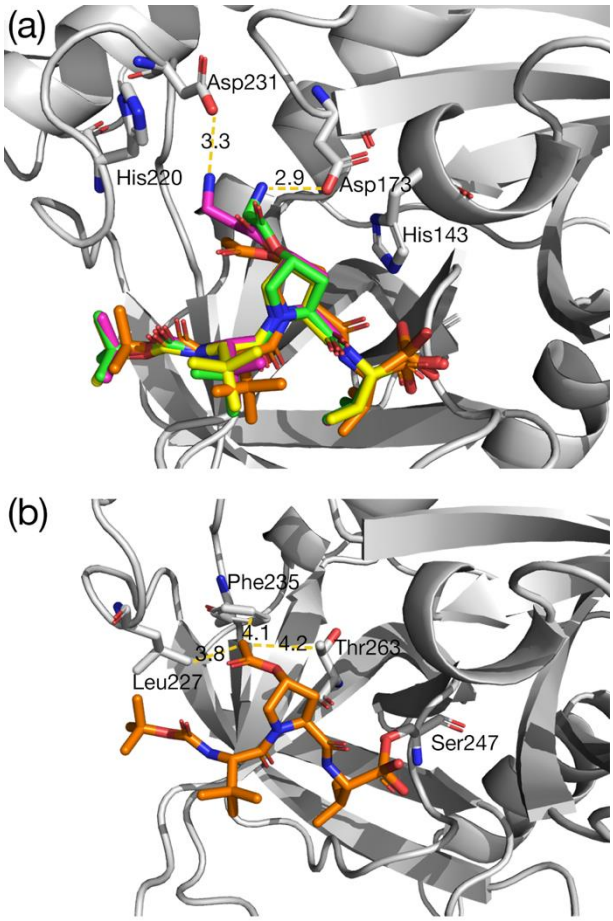

Fig. 6. (a) Superimposed docking positions of **2** (yellow), **25** (orange), **28** (green) and **29** (pink) and potential electrostatic interactions (yellow dashed lines) with aspartate residues at the S2 subpocket. (b) van der Waals interactions (yellow dashed lines) between the acetyl group of **25** (orange) and hydrophobic residues (shown in stick) at the CtHtrA active site (shown as a grey ribbon).

Interestingly, in contrast to our hypothesis that proline analogues with 4*R*-configured triazoles would impart better antichlamydial inhibitory activities, compound **49** with a 4*S*-substituted triazoyl group demonstrated the strongest inhibitory activity against *Chlamydia* in bacterial cell assays complemented by promising antiCtHtrA inhibition. A possible explanation is that while triazoyl moieties still exert a gauche effect, it is however, significantly weakened compared to that of the hydroxyl group by competing steric effects [58] and possibly intermolecular interactions with the protease residues. Based on the weaker preference for the analogous ring puckers in the case of the triazole moieties, compound **49** was docked against CtHtrA with an *exo*-puckered proline (**Fig. 7**). The top three docking poses of **49** were within 1.5 Å RMSD and

oriented the *tert*-butyl alcohol substituent of the triazole facing towards the S2 pocket. The *tert*-butyl alcohol group could form a hydrogen bond with Asp173 (3.1 Å) residue (**Fig. 7**), resulting in strong inhibition of CtHtrA (approximately 9-fold improvement in IC_{50} compared to **1**; **Table 2**) and *Chlamydia* in whole cell assays (**Fig. 5**). 4*S*-triazole-substituted proline analogues with an α-ketoamide covalent warhead have been found to be strong inhibitors of human HtrA1 in a recent patent for treating age-related macular degeneration [59]. This supports our findings that 4*S*-configuration is preferred with 4*S*-triazole-substituted proline analogues. Compound **1** has previously been shown to lack inhibitory activity against human HtrA1 [24], yet further selectivity testing might be needed for the triazole-substituted proline analogues.

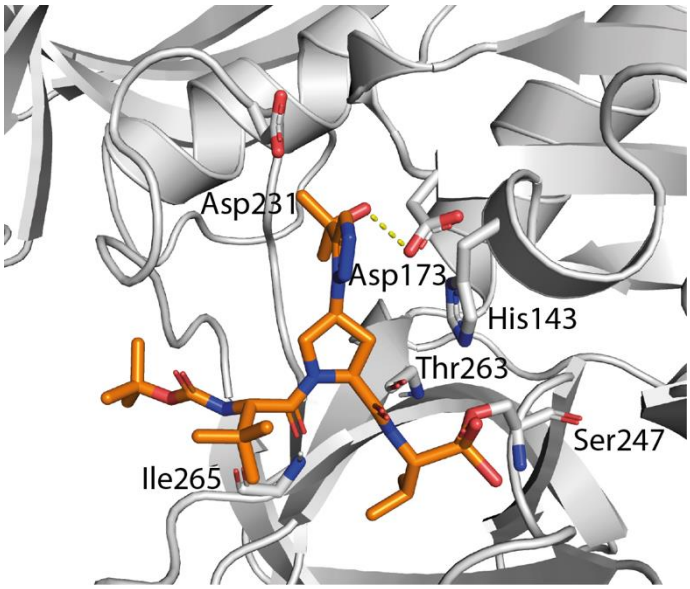

Fig. 7. Compound **49** (orange) was docked against the CtHtrA homology model. Hydrogen bonding (3.1 Å) between the tertiary alcohol of **49** and Asp173 is indicated by dashed yellow line. Key residues of the CtHtrA active site are shown in sticks.

3. Conclusions

Incorporation of unnatural amino acids into peptide analogues or peptidomimetics can augment molecular interactions with a biological target and improve metabolic stability (through resistance to proteolysis) and bioavailability, while maintaining selectivity and potency of therapeutic peptides. Herein, proline-editing was a key strategy in the optimization of lead tripeptides **1** and **2** against CtHtrA, which was carried out by pyrrolidine ring expansion and

Cγ-substitution with a diverse range of functional groups ranging from a simple hydroxyl group to mono- or di-substituted triazoyl moieties. In the first-generation proline-based analogues, compound **25** with an acetyl group incorporated at the Cγ-position of proline, increased the antiCtHtrA potency and selectivity over HNE by about 6-fold and 12-fold relative to **1**. Second-generation 4-substituted proline analogues were designed with triazoyl moieties in place of the acetyl group in **25** to improve antibacterial activities against *Chlamydia* cells as well as chemical stability. A library of substituted triazoles with different functional groups at either the C4' or C5' position was successfully synthesized with complete regioselectivity using CuI and $RuCp^*Cl(PPh_3)_2$ catalysed azide-alkyne cycloaddition click chemistry. Second-generation compounds **43** and **49** showed improved inhibitory activity against CtHtrA by 12- and 9-fold, respectively, compared to **1**. In addition, compound **49** showed improved selectivity over HNE by over 22-fold compared to **1**, and resulted in complete loss of infectious progeny at 25 μM, the lowest dose tested. The docking investigation of **49** against a CtHtrA homology model, suggested that the triazolyl group of the compound is likely to induce *exo*-puckering of proline possibly due to intermolecular H-bonding and the steric effects competing against the gauche relationship. All 4-substituted proline analogues as well as **19** were non-cytotoxic to HEp-2 cells and provide further opportunities for the identification of a narrow spectrum treatment for Chlamydia.

4. Experimental

4.1. General methods

All solvents and reagents were commercially procured (Sigma-Aldrich, Merck, AK Scientific, Thermo Scientific, Acros Organics, BDH, and Cambridge Isotope) and used without further purification. Organic solvent extracts were dried with $MgSO_{4(s)}$ and subjected to rotary evaporation, and finally dried at 10^{-1} mbar using a high vacuum pump. Silica gel 60 (0.040–0.063 mm, 200–400 mesh) was used for flash column chromatography with all solvent systems expressed as volume to volume (v/v) ratios. Analytical thin layer chromatography (TLC) was performed on Merck TLC aluminium plates coated with 0.2 mm silica gel 60 F254. Spots were generally detected by UV (254 nm) and/or permanganate staining. ^{1}H, ^{13}C and ^{31}P NMR spectra were recorded at room temperature on Varian 400 MHz spectrometers. Samples were prepared in deuterated solvents, chloroform (δ 7.26, 77.16 ppm), methanol (δ 3.31, 49.00 ppm) or acetonitrile (δ 1.95, 118.69 and 1.72 ppm) with the respective ^{1}H and ^{13}C chemical shifts shown

in brackets. Chemical shifts (δ) are expressed in parts per million (ppm) and coupling constants (*J*) in Hertz (Hz), both measured against the residual solvent peak. High resolution mass spectrometry was recorded on a Bruker microTOF-Q spectrometer with an electrospray ionization (ESI) source. The purity of compounds was determined by reverse-phase high performance liquid chromatography (HPLC) carried out on an Agilent HPLC with a Gemini 5 μm C18 110 column (250 Å ~4.6 mm, Phenomenex, New Zealand). Compounds were eluted using solvent A: 0.1% trifluoroacetic acid (TFA) in water and solvent B: 0.1% TFA in acetonitrile (ACN) over a linear gradient (**Table S9**). Compounds were detected at 254/210 nm with a flow rate of 1.0 mL/min. Optical rotation was recorded by using an Autopol IV polarimeter (Rudolph Research Analytical, USA). Final compounds including those obtained as isomeric mixtures, are >95% pure, see *supporting information* for HPLC traces of the compounds.

4.2. Synthesis and characterization of final compounds

Synthetic procedures and characterization of precursor compounds (**4**, **8**-**17**, **24**, **26**, **27**, **30**, **31**) are reported in the *supporting information.*

General procedure for peptide coupling to α-aminoalkyl phosphonate diphenyl esters (19-23, 25, 28, 29); Method A. To a solution of the hydrobromide salt of 1-aminoalkyl phosphonate diphenyl ester **18** (1.5 equiv.) in anhydrous DMF was added DIPEA (2.5 equiv.), and the reaction mixture was stirred for 10 min until complete dissolution was achieved. The acid precursor (1.0 equiv.) in anhydrous DMF was then added dropwise, followed by the addition of HBTU (1.2 equiv.). The reaction mixture was stirred at room temperature for 24 h. When the reaction was complete, the mixture was extracted with EtOAc (3 × 25 mL) and the combined organic layers were washed with saturated aqueous $NaHCO_3$ (3 × 25 mL), MilliQ water (3 × 25 mL) and then brine (3 × 25 mL). The organic layer was dried over $MgSO_{4(s)}$, filtered, concentrated *in vacuo* then purified by flash column chromatography (3:2 Hex:EtOAc, unless specified otherwise).

General procedure for CuI-catalyzed click chemistry to produce 1,4-disubstituted triazoles (34-37); Method B

To a solution of an azide (1 equiv.) in anhydrous THF was added an alkyne, DIPEA (10 equiv.) and CuI (2 equiv.) under $N_{2(g)}$ and stirred overnight at room temperature. The reaction mixture was adsorbed onto silica gel and subjected to flash chromatography for purification of the desired product. The C4' and C5' of the triazole group were not always visible in the ^{13}C NMR spectrum, but the presence of the triazole ring was confirmed by ^{1}H NMR and mass spectrometry. The C4' and C5' of the triazole group were not always visible in ^{31}C NMR, while the rest of the carbon peaks were detected. ^{1}H NMR and mass spectrometry confirmed that the desired triazole products were successfully formed.

General procedure for ruthenium-catalyzed click chemistry to produce 1,4,5- or 1,5-substituted triazoles (32, 33, 38-41); *Method C* [60]

To an azide (1 equiv.) solution in anhydrous dioxane was added an alkyne (1 equiv.) and $RuCp^*Cl(PPh_3)_2$ (0.05 equiv.) under $N_{2(g)}$ and the reaction mixture stirred at 60 °C overnight. The volatile solvent was evaporated *in vacuo* and the residue was purified by flash silica gel chromatography. The C4' and C5' of the triazole group were not always visible in the ^{13}C NMR spectrum, but the presence of the triazole ring was confirmed by ^{1}H NMR and mass spectrometry.

General procedure for the synthesis of 42-50 after the azide-alkyne cycloaddition reaction; Method D.

To a mixture of ester **32-40** in THF:H_2O (3:1) was added $LiOH.H_2O$ (5 equiv.) and the mixture stirred for 2 h at room temperature. The reaction mixture was acidified with 1 M HCl slowly to pH 1-2. The product was extracted with EtOAc (3 × 50 mL) and the combined organic fractions were washed with brine (50 mL), dried over $MgSO_{4(s)}$ and filtered. The product was concentrated *in vacuo* to obtain the acid product. Without further purification, the resulting acid was reacted with **18** according to Method A and purified using the specified protocol for the flash chromatography to afford the final compounds **42-50**.

***tert*-Butyl N-[(2*S*)-1-[(2*S*)-2-{[1-(diphenoxyphosphoryl)-2-methylpropyl]carbamoyl}piperidin-1-yl]-3,3-dimethyl-1-oxobutan-2-yl]carbamate (19).**

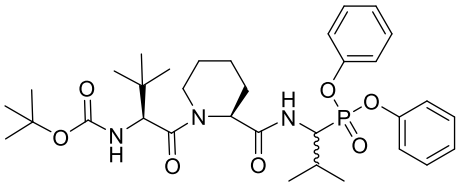

The hydrobromide salt of **18** (60.2 mg, 0.156 mmol) and DIPEA (68 μL, 0.390 mmol) in DMF (1 mL) was reacted with **13** (53.4 mg, 0.156 mmol) in DMF (1 mL) then HBTU (71.0 mg, 0.187 mmol). The reaction was purified as described in Method A above to obtain a colourless oil as a mixture of two diastereomers (46.4 mg, 0.074 mmol, 47%, R_f 0.58, 0.47, 2:1 PE:EtOAc). $[\alpha]_{589}^{21}$= +19.56 (*c* = 1.0, $CHCl_3$). ^{1}H NMR (400 MHz, $CDCl_3$) δ 7.34-1.01 (m, 10H, Phenoxy-H), 5.41-5.40 (m, 0.5H, 0.5 × -NH), 5.35-5.31 (m, 0.5H, 0.5 × -NH), 5.27-5.21 (m, 0.5H, 0.5 × -NH), 5.12-5.10 (m, 0.5H, 0.5 × -NH), 4.86-4.6 (m, 2.5H, 1 × Val-$_\alpha$H, 1 × Pip-$_\alpha$H, 0.5 × Tle-$_\alpha$H), 4.51-4.49 (m, 0.5H, 0.5 × Tle-$_\alpha$H), 4.15-3.98 (m, 1H, Pip-$_\varepsilon$H), 3.22-2.97 (m, 1H, Pip-$_\varepsilon$H), 2.48-2.30 (m, 2H, 1 × Val-$_\beta$H, 1 × Pip-H), 2.22-2.18 (m, 0.5H, 0.5H × Pip-H), 1.97-1.90 (m, 0.5H, 0.5H × Pip-H), 1.77-1.45 (m, 4H, 4 × Pip-H), 1.42-1.28 (m, 9H, ^{t}butyl), 1.13-0.92 (m, 15H, 6 × Val-$_\gamma$H, 9 × Tle-$_\gamma$H). ^{13}C NMR (101 MHz, $CDCl_3$) δ 173.3, 172.6, 170.8 (d, $J_{C\text{-}P}$= 6.0 Hz), 170.4 (d, $J_{C\text{-}P}$= 5.0 Hz), 156.0, 155.5, 150.5 (d, $J_{C\text{-}P}$= 10.1 Hz), 150.3 (d, $J_{C\text{-}P}$= 10.1 Hz), 129.99 (d, $J_{C\text{-}P}$= 1.0 Hz), 129.95 (d, $J_{C\text{-}P}$= 0.8 Hz), 129.9, 129.8, 125.6, 125.5, 125.39 (d, $J_{C\text{-}P}$= 1.3 Hz), 125.35 (d, $J_{C\text{-}P}$= 0.9 Hz), 125.3 d, $J_{C\text{-}P}$= 0.9 Hz), 125.2 d, $J_{C\text{-}P}$= 0.8 Hz), 121.99 (d, $J_{C\text{-}P}$= 3.8 Hz), 120.96 (d, $J_{C\text{-}P}$= 4.0 Hz), 120.9 (d, $J_{C\text{-}P}$= 4.5 Hz), 79.81, 79.78, 57.4, 57.0, 56.5, 56.1, 53.1, 52.3, 51.75 (d, $J_{C\text{-}P}$= 155.5 Hz), 50.8 (d, $J_{C\text{-}P}$= 153.5 Hz), 44.9, 44.5, 35.7, 35.1, 29.2 (d, $J_{C\text{-}P}$= 3.6 Hz), 29.0 (d, $J_{C\text{-}P}$= 3.8 Hz), 28.4, 28.3, 27.4, 26.9, 26.7, 26.1, 25.4, 25.1, 25.0, 20.7 (d, $J_{C\text{-}P}$= 14.3 Hz), 20.4 (d, $J_{C\text{-}P}$= 17.4 Hz), 18.0 (d, $J_{C\text{-}P}$= 4.4 Hz), 17.9 (d, $J_{C\text{-}P}$= 3.9 Hz). HRMS-ESI calculated for $C_{33}H_{48}N_3NaO_7P$ [M+Na^+] 652.3122, found *m/z* 652.3112. Analytical RP-HPLC (Table S9 for HPLC methods) t_R=36.54, 38.22 min.

***tert*-Butyl N-[(*2S*)-1-[(*2S,4S*)-2-{[1-(diphenoxyphosphoryl)-2-methylpropyl]carbamoyl}-4-phenylpyrrolidin-1-yl]-3,3-dimethyl-1-oxobutan-2-yl]carbamate (20).**

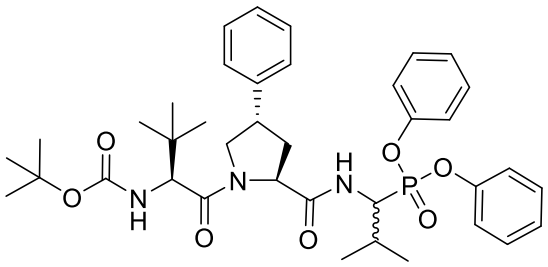

The hydrobromide salt of **18** (45.8 mg, 0.119 mmol) and DIPEA (43 μL, 0.247 mmol) in DMF (1 mL) was reacted with **14** (40.0 mg, 98.9 μmol) in DMF (1 mL) then HBTU (45.1 mg, 0.119 mmol). The reaction was purified as described in Method A above to obtain a colourless oil as a mixture of two diastereomers (38.7 mg, 56.9 μmol, 57%, R_f 0.50, 0.39, 3:2 n-Hex:EtOAc). $[\boldsymbol{\alpha}]_{589}^{21}$= -12.86 (*c* = 0.5, $CHCl_3$). ^{1}H NMR (400

MHz, $CDCl_3$) δ 7.52 (d, *J*= 9.4 Hz, 0.5H, 0.5 × -NH), 7.38 (d, *J*= 10.7 Hz, 0.5H, 0.5 × -NH), 7.40-7.09 (m, 15H, Phenyl-H), 5.32 (d, *J*= 8.0 Hz, 0.5H, 0.5 × -NH), 5.22 (d, *J*= 10.0 Hz, 0.5H, 0.5 × -NH), 4.92-4.90 (m, 0.5H, 0.5 × Pro-$_\alpha$H), 4.82-4.73 (m, 1H, Val-$_\alpha$H), 4.63-4.61 (m, 0.5H, 0.5 × Pro-$_\alpha$H), 4.33-4.28 (m, 1H, Tle-$_\alpha$H), 4.12-4.05 (m, 1H, Pro-$_\delta$H), 3.99-3.95 (m, 1H, Pro-$_\delta$H), 3.82-3.73 (m, 1H, Pro-$_\gamma$H), 2.78-2.74 (m, 1H, 0.5 × Pro-$_\beta$H), 2.49-2.37 (m, 1.5H, 0.5 × Pro-$_\beta$H, 1 × Val-$_\beta$H), 2.12-2.06 (m, 0.5H, 0.5 × Pro-$_\beta$H), 2.00-1.92 (m, 0.5H, 0.5 × Pro-$_\beta$H), 1.42 (s, 9H, ^{t}butyl), 1.04 (s, 3H, Val-$_\gamma$H), 1.09-1.06 (m, 3H, Val-$_\gamma$H), 1.03-0.94 (m, 9H, Tle-$_\gamma$H). ^{13}C NMR (101 MHz, $CDCl_3$) δ 173.1, 172.3, 171.2 (d, $J_{C\text{-}P}$= 6.0 Hz), 155.59, 155.56, 150.5 (d, $J_{C\text{-}P}$= 9.8 Hz), 150.2 (d, $J_{C\text{-}P}$= 10.1 Hz), 150.11 (d, $J_{C\text{-}P}$= 9.4 Hz), 150.07 (d, $J_{C\text{-}P}$= 9.1 Hz), 139.6, 139.3, 129.77 (d, $J_{C\text{-}P}$= 1.0 Hz), 129.76 (d, $J_{C\text{-}P}$= 1.2 Hz), 129.7 (d, $J_{C\text{-}P}$= 0.6 Hz), 129.6 (d, $J_{C\text{-}P}$= 0.7 Hz), 128.71, 128.68, 127.2, 127.14, 127.06, 125.3 (d, $J_{C\text{-}P}$= 0.9 Hz), 126.2 (d, $J_{C\text{-}P}$= 0.9 Hz), 125.1 (d, $J_{C\text{-}P}$= 0.8 Hz), 120.8 (d, $J_{C\text{-}P}$= 4.1 Hz), 120.7 (d, $J_{C\text{-}P}$= 4.0 Hz), 120.6 (d, $J_{C\text{-}P}$= 4.2 Hz), 120.3 (d, $J_{C\text{-}P}$= 4.3 Hz), 79.7, 79.6, 60.6, 60.2, 58.31, 58.27, 54.3, 54.2, 51.5 (d, $J_{C\text{-}P}$= 153.9 Hz), 51.2 (d, $J_{C\text{-}P}$= 155.4 Hz), 35.5, 35.2, 34.7, 34.5, 29.4 (d, $J_{C\text{-}P}$= 3.7 Hz), 29.3 (d, $J_{C\text{-}P}$= 3.8 Hz), 28.34, 28.31, 26.3, 26.2, 20.6 (d, $J_{C\text{-}P}$= 13.6 Hz), 20.3 (d, $J_{C\text{-}P}$= 13.9 Hz), 18.1 (d, $J_{C\text{-}P}$= 4.6 Hz), 17.9 (d, $J_{C\text{-}P}$= 4.2 Hz). ^{31}P NMR (162 MHz, $CDCl_3$) δ 17.36 (38.0%), 16.78 (62.0%). HRMS-ESI calculated for $C_{38}H_{50}N_3NaO_7P$ [M+Na^+] 714.3279, found *m/z* 714.3262. Analytical RP-HPLC (Table S9 for HPLC methods) t_R=40.28, 40.59 min.

***tert*-Butyl N-[(*2S*)-1-[(*2S,4S*)-4-cyclohexyl-2-{[1-(diphenoxyphosphoryl)-2-methylpropyl]carbamoyl}pyrrolidin-1-yl]-3,3-dimethyl-1-oxobutan-2-yl]carbamate (21).**

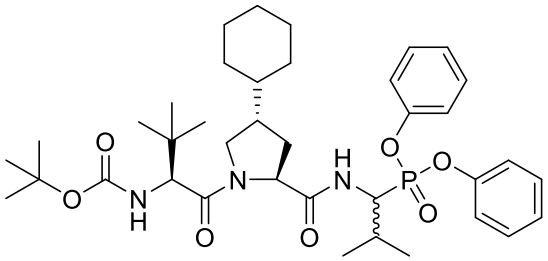

Compound **15** (0.11 g, 0.275 mmol), HBTU (0.13 g, 0.330 mmol), DIPEA (120 μL, 0.688 mmol) and the hydrobromide salt of **18** (0.13 g, 0.330 mmol) were reacted. The crude material was purified using flash silica gel column chromatography (3:1 PE:EtOAc) as described in Method A to yield the desired product as a white solid mixture of two diastereomers (0.16 g, 0.231 mmol, 84%, R_f 0.30, 3:1 PE:EtOAc). $[\alpha]_{589}^{21}$= -33.62 (*c* = 1.0, $CHCl_3$). ^{1}H NMR (400 MHz, $CDCl_3$) δ 7.47-7.12 (m, 11H, 1 × -NH, 10 × Phenoxy-H), 5.32-5.22 (m, 1H, -NH), 4.79-4.68 (m, 1H, Val-$_\alpha$H), 4.52-4.50 (m, 1H, Pro-$_\alpha$H), 4.32-4.25 (m, 1H, Tle-$_\alpha$H), 3.81-3.68 (m, 1H, Pro-$_\delta$H), 3.37-3.31 (m, 1H, Pro-$_\delta$H), 2.53-2.34 (m, 2H, 1 × Pro-$_\beta$H, 1 × Val-$_\beta$H), 2.27-2.22 (m,

1H, Pro-$_{\gamma}$H), 2.08-1.97 (m, 1H, Pro-$_{\beta}$H), 1.72-1.49 (m, 6H, cyclohexyl-H), 1.47-1.27 (m, 9H, ^{t}butyl), 1.21-0.85 (m, 20H, 5 × cyclohexyl-H, 9 × Tle-$_{\gamma}$H, 6 × Val-$_{\gamma}$H). ^{13}C NMR (101 MHz, $CDCl_3$) δ 173.0, 172.3, 171.5 (d, $J_{C\text{-}P}$= 5.5 Hz), 171.4 (d, $J_{C\text{-}P}$= 6.3 Hz), 155.60, 155.56, 150.4 (d, $J_{C\text{-}P}$= 9.9 Hz), 150.1 (d, $J_{C\text{-}P}$= 10.2 Hz), 150.2 (d, $J_{C\text{-}P}$= 9.4 Hz), 150.0 (d, $J_{C\text{-}P}$= 9.3 Hz), 129.77 (d, $J_{C\text{-}P}$= 0.8 Hz), 129.75 (d, $J_{C\text{-}P}$= 1.0 Hz), 129.7 (d, $J_{C\text{-}P}$= 0.6 Hz), 129.6 (d, $J_{C\text{-}P}$= 0.7 Hz), 125.3 (d, $J_{C\text{-}P}$= 0.9 Hz), 125.2 (d, $J_{C\text{-}P}$= 0.7 Hz), 125.1 (d, $J_{C\text{-}P}$= 0.5 Hz), 120.8 (d, $J_{C\text{-}P}$= 4.0 Hz), 120.7 (d, $J_{C\text{-}P}$= 4.1 Hz), 120.6 (d, $J_{C\text{-}P}$= 4.3 Hz), 120.4 (d, $J_{C\text{-}P}$= 4.4 Hz), 79.68, 79.65, 60.7, 60.3, 58.1, 58.0, 52.63, 52.57, 51.2 (d, $J_{C\text{-}P}$= 153.4 Hz), 51.1 (d, $J_{C\text{-}P}$= 155.1 Hz), 44.6, 44.4, 41.4, 41.2, 35.6, 35.3, 31.9, 31.7, 31.6, 31.28, 31.25, 29.3 (d, $J_{C\text{-}P}$= 4.2 Hz), 29.2 (d, $J_{C\text{-}P}$= 3.7 Hz), 28.34, 28.32, 26.3, 26.2, 26.1, 26.03, 25.98, 25.95, 25.9, 20.7 (d, $J_{C\text{-}P}$= 12.7 Hz), 20.3 (d, $J_{C\text{-}P}$= 13.9 Hz), 18.1 (d, $J_{C\text{-}P}$= 4.5 Hz), 17.9 (d, $J_{C\text{-}P}$= 4.3 Hz). ^{31}P NMR (162 MHz, $CDCl_3$), δ 17.54 (35.9%), 16.99 (64.1%). HRMS-ESI calculated for $C_{38}H_{56}N_3NaO_7P$ [M+Na^+] 720.3748, found *m/z* 720.3736. Analytical RP-HPLC (Table S9 for HPLC methods) t_R=47.08, 47.37 min.

tert-Butyl N-[(*2S*)-1-[(*2S,4S*)-2-{[1-(diphenoxyphosphoryl)-2-methylpropyl]carbamoyl}-4-hydroxypyrrolidin-1-yl]-3,3-dimethyl-1-oxobutan-2-yl]carbamate (22).

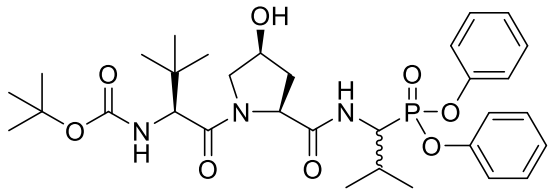

Compound **16** (0.18 g, 0.51 mmol), HBTU (0.21 g, 0.56 mmol), DIPEA (220 μL, 1.27 mmol) and the hydrobromide salt of **18** (0.22 g, 0.56 mmol) were reacted, then the crude material was purified using flash silica gel column chromatography (40-60% EtOAc in n-Hex) as described in the Method A to yield the desired product as a white solid mixture of two diastereomers (0.12 g, 0.18 mmol, 36%, R_f 0.33, 2:3 n-Hex:EtOAc). $[\boldsymbol{\alpha}]_{589}^{21}$= -37.22 (*c* = 1.0, $CHCl_3$). ^{1}H NMR (400 MHz, $CDCl_3$) δ 7.79 (br. s, 0.5H, 0.5 × -NH), 7.58 (d, *J*= 10.4 Hz, 0.5H, 0.5 × -NH), 7.30-7.06 (m, 10H, Phenoxy-H), 5.46 (d, *J*= 10.4 Hz, 0.5H, 0.5 × -NH), 5.38 (d, *J*= 9.6 Hz, 0.5H, 0.5 × -NH), 4.86-86-4.82 (m, 0.5H, 0.5 × Pro-$_{\alpha}$H), 4.76-4.61 (m, 1.5H, 0.5 × Pro-$_{\alpha}$H, 1 × Val-$_{\alpha}$H), 4.48-4.44 (m, 0.5H, 0.5 × Pro-$_{\gamma}$H), 4.38-4.35 (m, 0.5H, 0.5 × Pro-$_{\gamma}$H), 4.25 (d, *J*= 9.9 Hz, 0.5H, 0.5 × Tle-$_{\alpha}$H), 4.20 (d, *J*= 9.6 Hz, 0.5H, 0.5 × Tle-$_{\alpha}$H), 3.91-3.78 (m, 2H, Pro-$_{\delta}$H), 2.47-2.38 (m, 1H, Val-$_{\beta}$H), 2.34-2.30 (m, 0.5H, 0.5 × Pro-$_{\beta}$H), 2.21-2.14 (m, 0.5H, 0.5 × Pro-$_{\beta}$H), 2.07-1.94 (m, 1H, Pro-$_{\beta}$H), 1.39 (s, 9H, ^{t}butyl), 1.15-1.02 (m, 6H, Val-$_{\gamma}$H), 0.97-0.85 (m, 9H, Tle¬$_{\gamma}$H). ^{13}C NMR (101 MHz, $CDCl_3$) δ 173.8 (d, $J_{C\text{-}P}$= 6.7 Hz), 173.5 (d, $J_{C\text{-}P}$= 6.7

Hz), 173.1, 172.6, 155.89, 155.86, 150.1 (d, $J_{C\text{-}P}$= 8.7 Hz), 150.0 (d, $J_{C\text{-}P}$= 10.4 Hz), 130.0 (d, $J_{C\text{-}P}$= 2.9 Hz), 129.8, 125.6, 125.5, 125.4, 120.94 (d, $J_{C\text{-}P}$= 4.3 Hz), 120.92 (d, $J_{C\text{-}P}$= 3.8 Hz), 120.7 (d, $J_{C\text{-}P}$= 4.3 Hz), 120.4 (d, $J_{C\text{-}P}$= 3.9 Hz), 79.9, 79.8, 71.33, 71.28, 59.9, 58.6, 58.53, 58.47, 58.4, 52.0 (d, $J_{C\text{-}P}$= 154.5 Hz), 51.3 (d, $J_{C\text{-}P}$= 153.6 Hz), 38.7, 35.8, 35.6, 35.2, 29.4 (d, $J_{C\text{-}P}$= 3.5 Hz), 28.50, 28.48, 26.4, 26.2, 20.7 (d, $J_{C\text{-}P}$= 13.8 Hz), 20.5 (d, $J_{C\text{-}P}$= 14.0 Hz), 18.1 (d, $J_{C\text{-}P}$= 4.1 Hz), 17.9 (d, $J_{C\text{-}P}$= 4.4 Hz). ^{31}P NMR (162 MHz, $CDCl_3$) δ 17.06 (59.5%), 15.97 (40.5%). HRMS-ESI calculated for $C_{32}H_{46}N_3NaO_8P$ [M+Na^+] 654.2915, found *m/z* 654.2887. Analytical RP-HPLC (Table S9 for HPLC methods) t_R=25.95, 26.99 min.

***tert*-Butyl N-[(*2S*)-1-[(*2S*,*4R*)-2-{[1-(diphenoxyphosphoryl)-2-methylpropyl]carbamoyl}-4-hydroxypyrrolidin-1-yl]-3,3-dimethyl-1-oxobutan-2-yl]carbamate (23).**

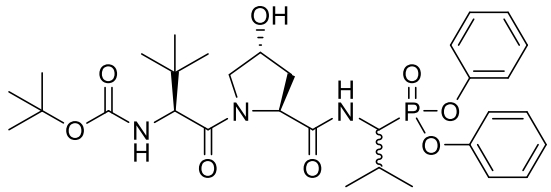

Compound **17** (0.94 g, 2.61 mmol), HBTU (1.09 g, 2.87 mmol), DIPEA (1.2 mL, 6.53 mmol) and the hydrobromide salt of **18** (1.10 g, 2.87 mmol) were reacted, then the crude material was purified using flash silica gel column chromatography (40-60% EtOAc in n-Hex) as described in the Method A to yield the desired product as a white solid mixture of two diastereomers (1.24 g, 1.97 mmol, 75%, R_f 0.33, 2:3 n-Hex:EtOAc). $[\boldsymbol{\alpha}]_{589}^{21}$= -56.20 (*c* = 1.0, $CHCl_3$). ^{1}H NMR (400 MHz, $CDCl_3$) δ 7.43 (d, *J*= 10.4 Hz, 0.5H, 0.5 × -NH), 7.31-7.12 (m, 10.5H, 10 × Phenoxy-H, 0.5 × -NH), 5.38 (d, *J*= 9.2 Hz, 0.5H, 0.5 × -NH), 5.27 (d, *J*= 9.2 Hz, 0.5H, 0.5 × -NH), 4.85 (t, *J*= 8.0 Hz, 0.5H, 0.5 × Pro-αH), 4.79-4.70 (m, 1H, Val-αH), 4.61 (t, *J*= 8.0 Hz, 0.5H, 0.5 × Pro-αH), 4.46-4.22 (m, 1H, Pro-γH), 4.22-4.17 (m, 1H, Tle-αH), 4.10-4.04 (m, 1H, Pro-δH), 3.61 (dd, *J*= 11.6, 3.6 Hz, 0.5H, 0.5 × Pro-δH), 3.44 (dd, *J*= 11.6, 3.6 Hz, 0.5H, 0.5 × Pro-δH), 2.46-2.36 (m, 1.5H, 1 × Val-βH, 0.5 × Pro-βH), 2.29-2.17 (m, 1H, Pro-βH), 2.03-1.96 (m, 0.5H, 0.5 × Pro-βH), 1.40 (s, 9H, ^{t}butyl), 1.14-1.12 (m, 3H, Val-γH), 1.07-1.04 (m, 3H, Val-γH), 0.99 (s, 4.5H, Tle¬γH), 0.91 (s, 4.5H, Tle-γH). ^{13}C NMR (101 MHz, $CDCl_3$) δ 173.3, 172.4, 171.43 (d, $J_{C\text{-}P}$= 6.7 Hz), 171.41 (d, $J_{C\text{-}P}$= 5.9 Hz), 156.7, 156.6, 150.5 (d, $J_{C\text{-}P}$= 9.9 Hz), 150.4, 150.22 (d, $J_{C\text{-}P}$= 9.5 Hz), 150.16 (d, $J_{C\text{-}P}$= 9.3 Hz), 129.92 (d, $J_{C\text{-}P}$= 1.0 Hz), 129.87 (d, $J_{C\text{-}P}$= 1.0 Hz), 129.85 (d, $J_{C\text{-}P}$= 0.8 Hz), 129.8 (d, $J_{C\text{-}P}$= 0.8 Hz), 125.4, 125.3, 121.0 (d, $J_{C\text{-}P}$= 4.1 Hz), 120.9 (d, $J_{C\text{-}P}$= 4.3 Hz), 120.8 (d, $J_{C\text{-}P}$= 4.2 Hz), 120.5 (d, $J_{C\text{-}P}$= 4.4 Hz), 80.6, 80.4, 70.2, 69.9, 58.94, 58.91, 58.80, 58.78, 56.7, 56.5, 51.5 (d, $J_{C\text{-}P}$= 155.0 Hz), 51.2 (d, $J_{C\text{-}P}$= 154.5 Hz), 36.6, 36.5, 35.2, 34.7, 29.5 (d, $J_{C\text{-}P}$= 4.0 Hz), 29.4 (d, $J_{C\text{-}P}$= 4.1 Hz), 28.5, 28.4, 26.5, 26.4, 20.7 (d,

$J_{C\text{-}P}$= 13.9 Hz), 20.5 (d, $J_{C\text{-}P}$= 13.9 Hz), 18.1 (d, $J_{C\text{-}P}$= 4.7 Hz), 18.0 (d, $J_{C\text{-}P}$= 4.2 Hz). ^{31}P NMR (162 MHz, $CDCl_3$) δ 17.36 (35.9%), 16.81 (64.1%). HRMS-ESI calculated for $C_{33}H_{46}N_3NaO_8P$ [M+Na^+] 654.2915, found *m/z* 654.2886. Analytical RP-HPLC (Table S9 for HPLC methods) t_R=25.60, 25.96 min.

***tert*-Butyl N-[(*2S*)-1-[(*2S,4R*)-2-{[1-(diphenoxyphosphoryl)-2-methylpropyl]carbamoyl}-4-(prop-1-en-2-yloxy)pyrrolidin-1-yl]-3,3-dimethyl-1-oxobutan-2-yl]carbamate (25).**

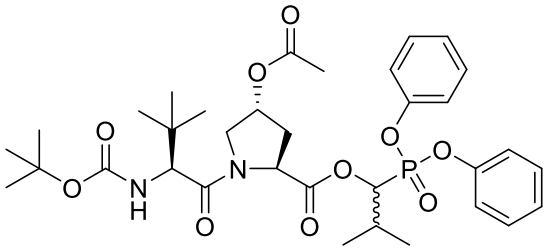

Compound **24** (115 mg, 0.298 mmol), HBTU (135 mg, 0.357 mmol), DIPEA (130 μL, 0.745 mmol) and the hydrobromide salt of **18** (173 mg, 0.447 mmol) were reacted, then the crude material was purified using flash silica gel column chromatography (1:1 n-Hex:EtOAc) as described in the Method A to yield a yellow oil as a mixture of two diastereomers (98 mg, 0.231 mmol, 49%, R_f 0.37, 1:1 n-Hex:EtOAc). $[\alpha]_{589}^{21}$= -32.40 (*c* = 0.5, $CHCl_3$). ^{1}H NMR (400 MHz, $CDCl_3$) δ 7.42-7.39 (m, 1H, -NH), 7.31-7.04 (m, 10H, Phenoxy-H), 5.55 (d, *J*= 10.0 Hz, 1H, -NH), 5.32-5.22 (m, 1H, Pro-$_\gamma$H), 4.89 (m, 0.5H, 0.5 × Pro-$_\alpha$H), 4.81-4.72 (m, 1H, Val-$_\alpha$H), 4.71-4.66 (m, 0.5H, 0.5 × Pro-$_\alpha$H), 4.26-4.19 (m, 1H, Tle-$_\alpha$H), 4.14-4.03 (m, 1H, Pro-$_\delta$H), 3.80 (dd, *J*= 11.8 Hz, 4.0 Hz, 0.5H, 0.5 × Pro-$_\delta$H), 3.64 (dd, *J*= 12.0, 4.4 Hz, 0.5H, 0.5 × Pro-$_\delta$H), 2.63-2.06 (m, 3H, 1 × Val-$_\beta$H, 2 × Pro-$_\beta$H), 2.04 (s, 1.5H, 0.5 × acetate-CH_3), 1.99 (s, 1.5H, 0.5 × acetate-CH_3), 1.41 (m, 9H, ^{t}butyl), 1.15-1.04 (m, 6H, Val-$_\gamma$H), 0.97 (s, 4.5H, Tle–$_\gamma$H), 0.87 (s, 4.5H, Tle–$_\gamma$H). ^{13}C NMR (101 MHz, $CDCl_3$) δ 172.9, 172.0, 171.3 (d, $J_{C\text{-}P}$= 6.8 Hz), 170.9 (d, $J_{C\text{-}P}$= 5.9 Hz), 170.6, 170.4, 155.8, 155.6, 150.3 (d, $J_{C\text{-}P}$= 9.6 Hz), 150.1 (d, $J_{C\text{-}P}$= 9.6 Hz), 150.0 (d, $J_{C\text{-}P}$= 9.5 Hz), 129.8 (d, $J_{C\text{-}P}$= 0.7 Hz), 129.74, 129.66 (d, $J_{C\text{-}P}$= 0.6 Hz), 125.34, 125.26, 125.2, 120.8 (d, $J_{C\text{-}P}$= 4.0 Hz), 120.7 (d, $J_{C\text{-}P}$= 4.4 Hz), 120.5 (d, $J_{C\text{-}P}$= 4.1 Hz), 120.3 (d, $J_{C\text{-}P}$= 4.2 Hz), 79.6, 79.5, 72.8, 72.3, 58.8, 58.7, 58.5, 54.0, 53.8, 51.4 (d, $J_{C\text{-}P}$= 154.8 Hz), 51.1 (d, $J_{C\text{-}P}$= 155.2 Hz), 35.7, 35.2, 33.9, 33.3, 29.29 (d, $J_{C\text{-}P}$= 4.2 Hz), 29.25 (d, $J_{C\text{-}P}$= 3.9 Hz), 28.34, 28.28, 26.3, 26.2, 20.9, 20.6 (d, $J_{C\text{-}P}$= 13.9 Hz), 20.3 (d, $J_{C\text{-}P}$= 13.9 Hz), 17.9 (d, $J_{C\text{-}P}$= 4.2 Hz). ^{31}P NMR (162 MHz, $CDCl_3$) δ 17.29 (40.2%), 16.69 (59.8%). HRMS-ESI calculated for $C_{34}H_{48}N_3NaO_9P$ [M+Na^+] 696.2967, found *m/z* 696.2986. Analytical RP-HPLC (Table S9 for HPLC methods) t_R=31.37, 31.92 min.

(*3R,5S*)-1-[(2S)-2-{[(*tert*-butoxy)carbonyl]amino}-3,3-dimethylbutanoyl]-5-{[1-(diphenoxyphosphoryl)-2-methylpropyl]carbamoyl}pyrrolidin-3-yl 2-aminoacetate (28).

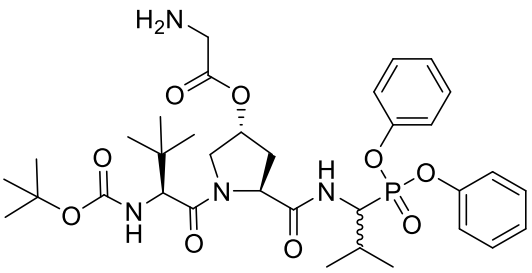

Compound **26** (0.28 g, 0.307 mmol) was reacted with 5% (v/v) piperidine (250 μL) in DMF (5 mL) at room temperature for 1-2 h and concentrated *in vacuo.* A portion of the crude was purified by semi preparative RP-HPLC then freeze-dried to obtain a white fluffy solid as a mixture of two diastereomers (1.7 mg, 2.365 μmol). $[\alpha]_{589}^{21}$= -24.48 (*c* = 0.5, MeOH). ^{1}H NMR (400 MHz, CD_3OD) δ 7.86 (d, *J*= 6.0 Hz, 0.5H, 0.5 × -NH), 7.71-7.68 (m, 0.5H, 0.5 × -NH), 7.48-7.10 (m, 11H, 10 × Phenoxy-H, 1 × -NH), 5.56-5.39 (m, 1H, Pro-$_\gamma$H), 4.73-4.61 (m, 2H, 1 × Pro-$_\alpha$H, 1 × Val-$_\alpha$H,), 4.21-4.13 (m, 2H, 1 × Tle-$_\alpha$H, 1 × Pro-$_\delta$H), 3.95-3.75 (m, 3H, 1 × Pro-$_\delta$H, C$\underline{H_2}$COO), 2.58-2.05 (m, 3H, 1 × 1 × Val-$_\beta$H, 2 × Pro-$_\beta$H), 1.43-1.38 (s, 9H, ^{t}butyl), 1.22-1.07 (m, 6H, Val-$_\gamma$H), 1.03-0.96 (m, 9H, Tle–$_\gamma$H). ^{13}C NMR (101 MHz, CD_3OD) δ 175.31 (d, $J_{C\text{-}P}$= 6.1 Hz), 174.25, 174.2, 169.6, 169.5, 159.32, 159.30, 152.8, 152.6 (d, $J_{C\text{-}P}$= 9.3 Hz), 132.3, 132.2, 132.0, 128.0 (d, $J_{C\text{-}P}$= 2.8 Hz), 127.93, 127.86 (d, $J_{C\text{-}P}$= 1.3 Hz), 123.6 (d, $J_{C\text{-}P}$= 4.0 Hz), 123.5 (d, $J_{C\text{-}P}$= 4.1 Hz), 122.9 (d, $J_{C\text{-}P}$= 4.1 Hz), 122.8 (d, $J_{C\text{-}P}$= 4.1 Hz), 81.9, 77.82, 77.78, 61.9, 61.8, 61.24, 61.20, 56.29, 56.26, 54.3 (d, $J_{C\text{-}P}$= 155.2 Hz), 53.5 (d, $J_{C\text{-}P}$= 155.0 Hz), 42.4, 37.42, 37.39, 37.3, 36.8, 31.9 (d, $J_{C\text{-}P}$= 3.2 Hz), 31.9 (d, $J_{C\text{-}P}$= 3.7 Hz), 30.0, 28.18, 28.14, 22.21 (d, $J_{C\text{-}P}$= 11.6 Hz), 22.18 (d, $J_{C\text{-}P}$= 12.3 Hz), 20.3 (d, $J_{C\text{-}P}$= 7.1 Hz), 20.0 (d, $J_{C\text{-}P}$= 6.0 Hz). ^{31}P NMR (162 MHz, $CDCl_3$) δ 17.91 (31.4%), 17.48 (68.6%). HRMS-ESI calculated for $C_{34}H_{49}N_4NaO_9P$ [M+Na^+] 711.3129, found *m/z* 711.3102. Analytical RP-HPLC (Table S9 for HPLC methods) t_R=13.98, 14.26 min.

(*3R,5S*)-1-[(*2S*)-2-{[(*tert*-butoxy)carbonyl]amino}-3,3-dimethylbutanoyl]-5-{[1-(diphenoxyphosphoryl)-2-methylpropyl]carbamoyl}pyrrolidin-3-yl 3-aminopropanoate (29).

Compound **27** (0.26 g, 0.281 mmol) was reacted with 5% (v/v) piperidine (250 μL) in DMF (5 mL) for 1-2 h and concentrated *in vacuo.* A portion of the resulting crude was purified by RP-

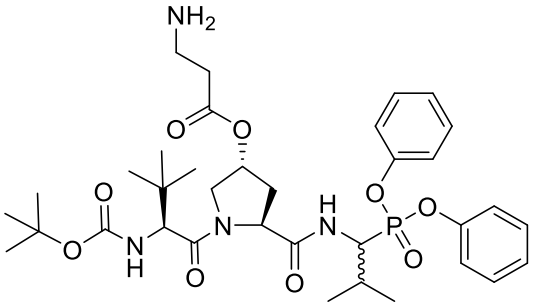

HPLC to obtain a white fluffy solid as a mixture of two diastereomers (5.23 mg, 7.431 μmol). $[\alpha]_{589}^{21}$= -16.44 (*c* = 0.5, MeOH). ^{1}H NMR (400 MHz, CD_3OD) δ 7.87 (d, *J*= 7.6 Hz, 0.5H, 0.5 × -NH), 7.69 (d, *J*= 7.2 Hz, 0.5H, 0.5 × -NH), 7.42-7.09 (m, 10H, Phenoxy-H), 5.45-5.33 (m, 2H, 1 × Pro-$_\gamma$H, 1 × -NH), 4.70-4.59 (m, 2H, 1 × Pro-$_\alpha$H, 1 × Val-$_\alpha$H), 4.17-4.09 (m, 2H, 1 × Tle-$_\alpha$H, 1 × Pro-$_\delta$H), 3.96-3.85 (m, 1H, Pro-$_\delta$H), 3.25-3.14 (m, 2H, -NHC$\underline{H_2}$), 2.77-2.71 (m, 2H, -$NH_2CH_2C\underline{H_2}$), 2.56-2.03 (m, 3H, 1 × 1 × Val-$_\beta$H, 2 × Pro-$_\beta$H), 1.41 (s, 9H, ^{t}butyl), 1.19-1.06 (m, 6H, Val-$_\gamma$H), 1.00-0.95 (m, 9H, Tle–$_\gamma$H). ^{13}C NMR (101 MHz, CD_3OD) δ 174.2 (d, $J_{C\text{-}P}$=6.7 Hz), 172.94, 172.86, 171.9, 171.8, 158.1, 151.6 (d, $J_{C\text{-}P}$= 10.1 Hz), 151.4 (d, $J_{C\text{-}P}$= 9.5 Hz), 151.1 (d, $J_{C\text{-}P}$= 10.9 Hz), 131.0 (d, $J_{C\text{-}P}$=1.5 Hz), 130.9 (d, $J_{C\text{-}P}$=0.9 Hz), 130.8, 126.8, 126.7, 126.6, 122.3 (d, $J_{C\text{-}P}$= 3.7 Hz), 122.3 (d, $J_{C\text{-}P}$= 3.7 Hz), 121.7 (d, $J_{C\text{-}P}$= 3.9 Hz), 121.5 (d, $J_{C\text{-}P}$= 4.2 Hz), 80.6, 75.5, 75.4, 60.54, 60.49, 60.09, 60.06, 55.1, 55.0, 53.1 (d, $J_{C\text{-}P}$= 155.8 Hz), 52.2 (d, $J_{C\text{-}P}$= 154.2 Hz), 36.3, 36.24, 36.20, 35.7, 32.27, 32.26, 30.7 (d, $J_{C\text{-}P}$= 3.5 Hz), 30.6 (d, $J_{C\text{-}P}$= 3.8 Hz), 28.7, 26.93, 26.90, 21.97 (d, $J_{C\text{-}P}$= 11.9 Hz), 20.96 (d, $J_{C\text{-}P}$= 11.9 Hz), 19.0 (d, $J_{C\text{-}P}$= 7.1 Hz), 18.8 (d, $J_{C\text{-}P}$= 6.0 Hz). ^{31}P NMR (162 MHz, $CDCl_3$) δ 17.92 (28.7%), 17.51 (71.3%). HRMS-ESI calculated for $C_{35}H_{51}N_4NaO_9P$ [M+Na^+] 725.3286, found *m/z* 725.3305. Analytical RP-HPLC (Table S9 for HPLC methods) t_R=13.42, 13.69 min.

Methyl (4*R*)-4-[4,5-bis(hydroxymethyl)-1H-1,2,3-triazol-1-yl]-1-[(2*S*)-2-{[(*tert*-butoxy)carbonyl]amino}-3,3-dimethylbutanoyl]p yrrolidine-2-carboxylate (32).

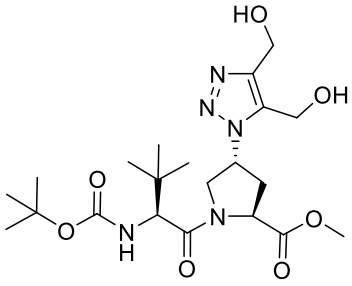

Compound **31** (61.6 mg, 0.161 mmol), 2-butyne-1,4-diol (55.3 mg, 0.643 mmol) and $RuCp^*Cl(PPh_3)_2$ (6.4 mg, 8.01 μmol) were reacted in dioxane (2 ml) as described in Method C and purified by flash chromatography (4:1 to 100:0 EtOAc:n-Hex, followed by 1:9 methanol:EtOAC) to yield a brown oil as a mixture of rotamers (64.0 mg, 0.136 mmol, 85%, R_f 0.11 in 100% EtOAc). ^{1}H NMR (400 MHz, $CDCl_3$) δ 5.27 (d, *J*= 9.6 Hz, 1H, -NH), 5.03-4.95 (m, 1H, Pro-$_\gamma$H), 4.82-4.62 (m, 5H, 1 × Pro-$_\alpha$H, 2 × C$\underline{H_2}$OH), 4.41-4.37 (m, 1H, Pro-$_\delta$H) 4.14-4.01 (m, 2H, 1 × Tle-$_\alpha$H, 1 × Pro-$_\delta$H), 3.76 (s, 3H, O-CH_3), 3.72 (s, br s, 2H, 2 × -OH), 3.18-3.13 (m, 1H, Pro-$_\beta$H), 2.51-2.45 (m, 1H, Pro-$_\beta$H), 1.33 (m, 9H, ^{t}butyl), 0.99 (m, 9H, Tle–$_\gamma$H). ^{13}C NMR (101 MHz,

$CDCl_3$) δ 172.0, 170.6, 156.0, 80.1, 58.3, 58.0, 57.8, 55.2, 52.5, 51.8, 50.7, 35.6, 33.9, 28.3, 26.2. HRMS-ESI calculated for $C_{21}H_{35}N_5O_7$ [M+Na^+] 492.2429, found *m/z* 492.2420.

Methyl (4*S*)-4-[4,5-bis(hydroxymethyl)-1H-1,2,3-triazol-1-yl]-1-[(2*S*)-2-{[(*tert*-butoxy)carbonyl]amino}-3,3-dimethylbutanoyl]p yrrolidine-2-carboxylate (33)

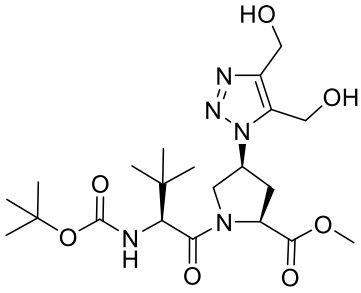

Compound **30** (0.10 g, 0.269 mmol), 2-butyne-1,4-diol (92.5 mg, 1.07 mmol) and $RuCp^*Cl(PPh_3)_2$ (10.7 mg, 13.4 μmol) in dioxane (2 ml) were reacted as described in Method C and purified using flash chromatography with 4:1 to 100:0 EtOAc:n-Hex, followed by 1:9 methanol:EtOAc to elute the title compound, which was obtained as a brown oil (71.0 mg, 0.151 mmol, 56%, R_f 0.49 in 4:1 EtOAc: n-Hex). ^{1}H NMR (400 MHz, $CDCl_3$) δ 5.33 (d, *J*= 9.6 Hz, 1H, -NH), 5.20-5.11 (m, 1H, Pro-$_\gamma$H), 4.80-4.63 (m, 5H, 1 × Pro-$_\alpha$H, 2 × C$\underline{H_2}$OH), 4.56-4.51 (m, 1H, Pro-$_\delta$H), 4.22 (d, *J*= 10 Hz, 1H, Tle-$_\alpha$H), 4.08-4.04 (m, 1H, Pro-$_\delta$H), 3.93 (s, br s, 2H, 2 × -OH), 3.74 (s, 3H, O-CH_3), 2.87-2.71 (m, 2H, Pro-$_\beta$H), 1.41 (s, 9H, ^{t}butyl), 1.02 (s, 9H, Tle–$_\gamma$H). ^{13}C NMR (101 MHz, $CDCl_3$) δ. 171.00, 170.95, 156.0, 132.0, 128.7, 80.0, 58.7, 57.5, 56.5, 55.0, 52.5, 52.1, 51.8, 35.8, 34.0, 28.4, 26.2. HRMS-ESI calculated for $C_{21}H_{35}N_5NaO_7$ [M+Na^+] 492.2429, found *m/z* 492.2424.

Methyl (4*R*)-1-[(2*S*)-2-{[(*tert*-butoxy)carbonyl]amino}-3,3-dimethylbutanoyl]-4-[4-(2-hydroxypropan-2-yl)-1H-1,2,3-triazol-1-yl]pyrrolidine-2-carboxylate (34).

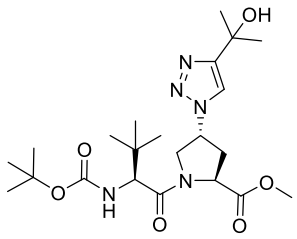

Compound **31** (45.3 mg, 0.118 mmol), 2-methyl-3-butyn-2-ol (19.9 mg, 0.236 mmol), DIPEA (0.31 g, 2.36 mmol) and CuI (45.0 mg, 0.236 mmol) were reacted in THF (1 mL) using Method B and purified by flash chromatography in 100% EtOAc to yield a white solid (53.0 mg, 0.113 mmol, 96%). ^{1}H NMR (400 MHz, $CDCl_3$) δ 7.73 (s, 1H, triazolyl-H), 5.36-5.32 (m, 1H, Pro-$_\gamma$H), 5.13 (d, *J*=9.2 Hz, 1H, -NH), 4.69 (t, *J*= 7.6 Hz, 1H, Pro-$_\alpha$H), 4.36-4.33 (m, 1H, Pro-$_\delta$H), 4.24-4.20 (m, 1H, Pro-$_\delta$H), 4.12 (d, *J*= 9.2 Hz, 1H, Pro-$_\delta$H), 3.75 (s, 3H, O-CH_3), 2.83-2.77 (m, 1H, Pro-$_\beta$H), 2.55-2.48 (m, 1H, Pro-$_\beta$H), 2.30 (br s, 1H, OH), 1.61 (s, 6H, C(C$\underline{H_3}$)$_2$OH), 1.40 (s, 9H,^{t}butyl), 1.05 (s, 9H, Tle–$_\gamma$H). ^{13}C NMR (101 MHz, $CDCl_3$) δ 171.7, 171.0, 156.1, 117.9, 80.1, 68.5, 59.02, 58.97, 57.6, 52.6, 52.5, 35.3,

35.2, 30.5, 28.3, 26.4. HRMS-ESI calculated for $C_{22}H_{37}N_5NaO_6$ [M+Na^+] 490.26360, found *m/z* 490.26449.

Methyl (2*S*,4*R*)-1-[(2*S*)-2-{[(*tert*-butoxy)carbonyl]amino}-3,3-dimethylbutanoyl]-4-[4-(hydroxymethyl)-1H-1,2,3-triazol-1-yl]pyrrolidine-2-carboxylate (35).

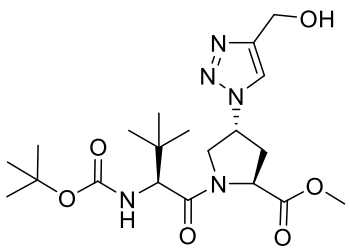

Compound **31** (47.7 mg, 0.124 mmol), propargyl alcohol (14.0 mg, 0.249 mmol), DIPEA (0.32 g, 2.49 mmol) and CuI (47.4 mg, 0.249 mmol) were reacted in THF (2 mL) using Method B and purified using flash chromatography in EtOAc with gradient increase of methanol up to 10% to yield a colourless oil (32.4 mg, 73.7 μmol, 59%). ^{1}H NMR (400 MHz, $CDCl_3$) δ 7.96 (br s, 1H, triazolyl-H), 5.35 (br s, 1H, -NH), 5.22-5.14 (m, 1H, Pro-$_\gamma$H), 4.78 (br s, 2H, C$\underline{H_2}$OH), 4.63 (t, *J*= 8.0 Hz, 1H, Pro-$_\alpha$H), 4.47-4.44 (m, 1H, Pro-$_\delta$H), 4.24-4.20 (m, 1H, Pro-$_\delta$H), 4.14 (d, *J*= 9.6 Hz, 1H, Tle-$_\alpha$H), 3.75 (s, 3H, O-CH_3), 2.87-2.82 (m, 1H, Pro-$_\beta$H), 2.54-2.48 (m, 1H, Pro-$_\beta$H), 2.16 (br s, 1H, -OH), 1.40 (s, 9H, ^{t}butyl), 1.05 (s, 9H, Tle–$_\gamma$H). ^{13}C NMR (101 MHz, $CDCl_3$) δ 171.6, 171.2, 156.3, 80.2, 59.0, 58.2, 57.5, 56.3, 52.6, 52.5, 35.4, 35.0, 28.3, 26.3. HRMS-ESI calculated for $C_{20}H_{33}N_5NaO_6$ [M+Na^+] 462.23230, found *m/z* 462.23210.

Methyl (2*S*,4*S*)-1-[(2*S*)-2-{[(*tert*-butoxy)carbonyl]amino}-3,3-dimethylbutanoyl]-4-[4-(hydroxymethyl)-1H-1,2,3-triazol-1-yl]pyrrolidine-2-carboxylate (36).

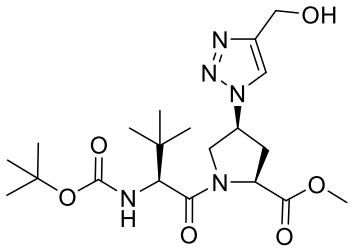

Compound **30** (50.7 mg, 0.132 mmol), propargyl alcohol (15 μL, 0.264 mmol), DIPEA (0.34 g, 2.64 mmol) and CuI (50.3 mg, 0.264 mmol) in THF (2 mL) were reacted using Method B and purified using flash chromatography in 1:4 to 0:100 n-Hex:EtOAc, followed by gradient addition of methanol up to 20% in EtOAc to yield a colourless oil (53 mg, 0.121 mmol, 91%). ^{1}H NMR (400 MHz, $CDCl_3$) δ 7.66 (s, 1H, triazolyl-H), 5.25 (br s, 1H, -NH), 5.19-5.11 (m, 1H, Pro-$_\gamma$H), 4.76 (br s, 2H, C$\underline{H_2}$OH), 4.68 (t, *J*= 8.0 Hz, 1H, Pro-$_\alpha$H), 4.61-4.56 (m, 1H, Pro-$_\delta$H), 4.22 (d, *J*= 9.6 Hz, 1H, Tle-$_\alpha$H), 4.03-3.98 (m, 1H, Pro-$_\delta$H), 3.75 (s, 3H, O-CH_3), 2.96-2.85 (m, 1H, Pro-$_\beta$H), 2.66-2.58 (m, 1H, Pro-$_\beta$H), 1.40 (s, 9H, ^{t}butyl), 1.01 (s, 9H, Tle–$_\gamma$H). ^{13}C NMR (101 MHz, $CDCl_3$) δ

171.2, 171.1, 155.9, 121.2, 79.9, 58.7, 57.9, 57.4, 56.3, 52.5, 52.4, 35.6, 34.2, 28.3, 26.2. HRMS-ESI calculated for $C_{20}H_{33}N_5NaO_6$ [M+Na^+] 462.23230, found *m/z* 462.23112.

Methyl (4*R*)-1-[(2*S*)-2-{[(*tert*-butoxy)carbonyl]amino}-3,3-dimethylbutanoyl]-4-(4-carbamoyl-1H-1,2,3-triazol-1-yl)pyrrolidine-2-carboxylate (37).

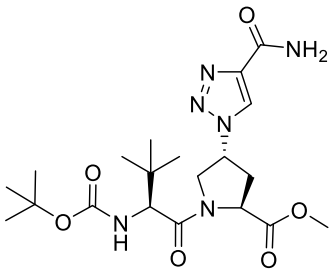

Compound **31** (45.0 mg, 0.117 mmol), propiolamide (16.2 mg, 0.235 mmol), DIPEA (0.30 g, 2.35 mmol) and CuI (44.8 mg, 0.235 mmol) were reacted as described in Method B, except that an equal volume of DMF was added to THF (total 2 mL) to solubilize the alkyne. Purification was conducted by flash chromatography in EtOAc with gradient increase of methanol up to 20% to yield a white solid (40.0 mg, 88.3 μmol, 75%, R_f 0.25 in 100% EtOAc). ^{1}H NMR (400 MHz, $CDCl_3$) δ 8.39 (s, 1H, triazolyl-H), 7.02 (br s, 1H, triazolyl-CONH), 5.91 (br s, 1H, triazolyl-CONH), 5.38-5.34 (m, 1H, Pro-$_\gamma$H), 5.16 (d, *J*= 9.6 Hz, 1H, -NH), 4.74 (t, *J*= 8.0 Hz, 1H, Pro-$_\alpha$H), 4.49-4.45 (m, 1H, Pro-$_\delta$H), 4.30-4.26 (m, 1H, Pro-$_\delta$H), 4.16 (d, *J*= 9.6 Hz, 1H, Tle-$_\alpha$H), 3.76 (s, 3H, O-CH_3), 2.86-2.80 (m, 1H, Pro-$_\beta$H), 2.60-2.54 (m, 1H, Pro-$_\beta$H), 1.38 (s, 9H, ^{t}butyl), 1.04 (s, 9H, Tle–$_\gamma$H). ^{13}C NMR (101 MHz, $CDCl_3$) δ 171.6, 171.2, 161.5, 156.0, 143.0, 124.8, 80.2, 59.3, 58.8, 57.5, 52.6, 52.4, 35.11, 35.07, 28.2, 26.3. HRMS-ESI calculated for $C_{20}H_{32}N_6NaO_6$ [M+Na^+] 475.22755, found *m/z* 475.22798.

Methyl (4*R*)-1-[(2*S*)-2-{[(*tert*-butoxy)carbonyl]amino}-3,3-dimethylbutanoyl]-4-[5-(2-hydroxypropan-2-yl)-1H-1,2,3-triazol-1-yl]pyrrolidine-2-carboxylate (38).

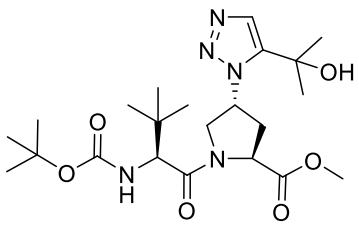

Compound **31** (84.0 mg, 0.219 mmol), 2-methyl-3-butyn-2-ol (73.7 mg, 0.876 mmol), and RuCp*Cl(PPh_3)$_2$ (8.7 mg, 11.0 μmol) in anhydrous dioxane (2 mL) were reacted as described in Method C and purified by flash chromatography with 30% PE in EtOAc to obtain a yellow oil as a mixture of rotamers (76 mg, 0.162 mmol, 74%). ^{1}H NMR (400 MHz, $CDCl_3$) δ 7.43 (s, 1H, triazolyl-H), 5.72 (br s, 1H, Pro-$_\gamma$H), 5.19 (d, *J*= 9.6 Hz, 1H, -NH), 5.00 (t, *J*= 7.4 Hz, 1H, Pro-$_\alpha$H), 4.34-4.30 (m, 1H, Pro-$_\delta$H), 4.14-4.06 (m, 2H, 1 × Pro-$_\delta$H, 1 × Tle-$_\alpha$H), 3.75 (s, 3H, O-CH_3), 3.51 (s, br s, 1H, -OH), 3.11-3.05 (m, 1H, Pro-$_\beta$H), 2.46-2.39 (m, 1H, Pro-$_\beta$H), 1.69 (s, 3H, C$\underline{H_3}$COH), 1.62 (s, 3H,

C<u>H$_3$</u>COH), 1.35 (s, 9H, ^{t}butyl), 0.98 (s, 9H, Tle–$_\gamma$H). ^{13}C NMR (101 MHz, $CDCl_3$) δ 172.2, 171.9, 171.4, 170.5, 155.7, 155.2, 79.9, 79.2, 67.4, 67.1, 59.5, 58.30, 58.27, 58.1, 54.1, 53.2, 52.8, 52.4, 37.2, 36.2, 35.7, 34.8, 30.8, 30.0, 28.3, 26.1. HRMS-ESI calculated for $C_{22}H_{37}N_5NaO_6$ [M+Na$^+$] 490.26360, found *m/z* 490.26282.

Methyl (4*S*)-1-[(2*S*)-2-{[(*tert*-butoxy)carbonyl]amino}-3,3-dimethylbutanoyl]-4-[5-(2-hydroxypropan-2-yl)-1H-1,2,3-triazol-1-yl]pyrrolidine-2-carboxylate (39).

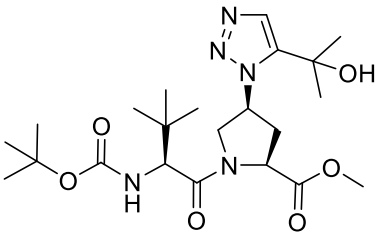

Compound **30** (0.10 g, 0.271 mmol), 2-methyl-3-butyn-2-ol (0.11 g, 1.36 mmol), and RuCp*Cl(PPh_3)$_2$ (10.8 mg, 13.6 μmol) in anhydrous dioxane (2 mL) were reacted as described in Method C and purified by flash chromatography with 3:7 PE:EtOAc to obtain a yellow oil (84.8 mg, 0.181 mmol, 67%, R_f 0.39 in 7:3 EtOAc: PE). ^{1}H NMR (400 MHz, $CDCl_3$) δ 7.44 (s, 1H, triazolyl-H), 5.77-5.64 (m, 1H, Pro-$_\gamma$H), 5.25 (d, *J*= 9.6 Hz, 1H, -NH), 4.70 (t, *J*= 8.4 Hz, 1H, Pro-$_\alpha$H), 4.54-4.50 (m, 1H, Pro-$_\delta$H), 4.20 (d, *J*=10 Hz, 1H, Tle-$_\alpha$H), 4.08-4.04 (m, 1H, Pro-$_\delta$H), 3.76 (s, 3H, O-CH_3), 3.06 (br s, 1H, OH), 2.83-2.79 (m, 2H, Pro-$_\beta$H), 1.68 (s, 3H, C<u>H$_3$</u>COH), 1.65 (s, 3H, C<u>H$_3$</u>COH), 1.39 (s, 9H, ^{t}butyl), 1.01 (s, 9H, Tle–$_\gamma$H). ^{13}C NMR (101 MHz, $CDCl_3$) δ 171.0, 155.8, 143.8, 130.1, 79.8, 67.6, 58.6, 57.5, 56.9, 52.9, 52.4, 35.7, 34.5, 30.7, 30.6, 28.3, 26.2. HRMS-ESI calculated for $C_{22}H_{37}N_5O_6$ [M+Na$^+$] 490.26360, found *m/z* 490.26204.

Methyl (4*R*)-1-[(2*S*)-2-{[(*tert*-butoxy)carbonyl]amino}-3,3-dimethylbutanoyl]-4-(5-carbamoyl-1H-1,2,3-triazol-1-yl)pyrrolidine-2-carboxylate (40).

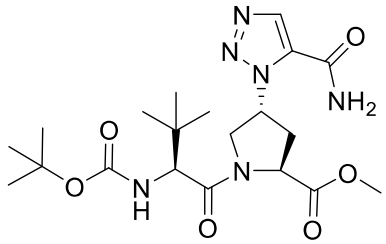

Compound **31** (48.0 mg, 0.125 mmol), propiolamide (35.0 mg, 0.501 mmol), and RuCp*Cl(PPh_3)$_2$ (5.0 mg, 6.26 μmol) were reacted as described in Method C, except that DMF was used as a reaction solvent instead of dioxane to solubilize propiolamide. The crude was purified by flash chromatography with 1:1 to 100:0 EtOAc:n-Hex, followed by gradient increase of methanol up to 20% in EtOAc to obtain the product as a yellow oil (43 mg, 98.1 μmol, 35%, R_f 0.27 in 1:1 EtOAc: n-Hex). ^{1}H NMR (400 MHz, $CDCl_3$) δ 8.37 (s, 1H, triazolyl-H), 7.01 (br s, 1H, triazolyl-CONH), 5.81 (br s, 1H, triazolyl-CONH), 5.40-5.34 (m, 1H, Pro-$_\gamma$H), 5.15 (d, *J*= 9.6

Hz, 1H, -NH),4.76 (t, *J*= 7.6 Hz, 1H, Pro-$_{\alpha}$H), 4.49-4.46 (m, 1H, Pro-$_{\delta}$H), 4.30-4.26 (m, 1H, Pro-$_{\delta}$H), 4.15 (d, *J*= 9.2 Hz, 1H, Tle-$_{\alpha}$H), 3.76 (s, 3H, O-CH_3), 2.87-2.80 (m, 1H, Pro-$_{\beta}$H), 2.60-2.54 (m, 1H, Pro-$_{\beta}$H), 1.39 (s, 9H, ^{t}butyl), 1.04 (s, 9H, Tle–$_{\gamma}$H). ^{13}C NMR (101 MHz, $CDCl_3$) δ 171.6, 171.2, 161.5, 156.0, 143.1, 124.8, 80.2, 59.3, 58.8, 57.5, 52.6, 52.4, 35.13, 35.09, 28.3, 26.3. HRMS-ESI calculated for $C_{20}H_{32}N_6NaO_6$ [M+Na^+] 475.22755, found *m/z* 475.22776.

Methyl (2*S*,4*S*)-1-[(2*S*)-2-{[(*tert*-butoxy)carbonyl]amino}-3,3-dimethylbutanoyl]-4-[4-(hydroxymethyl)-1H-1,2,3-triazol-1-yl]pyrrolidine-2-carboxylate (41).

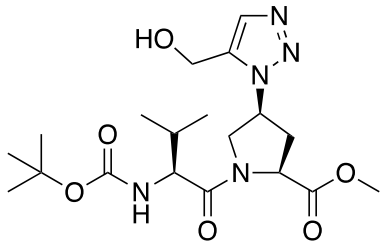

Compound **30** (65.5 mg, 0.149 mmol), propargyl alcohol (35 μL, 0.596 mmol), and $RuCp^*Cl(PPh_3)_2$ (5.9 mg, 7.45 μmol) in dioxane (2 mL) were reacted using Method C and purified using flash chromatography in 1:4 to 0:100 n-Hex:EtOAc to yield a colourless oil (53 mg, 0.121 mmol, 91%). ^{1}H NMR (400 MHz, $CDCl_3$) δ 7.62 (s, 1H, triazolyl-H), 5.27 (d, *J*= 9.6 Hz, 1H, -NH), 5.15-5.06 (m, 1H, Pro-$_{\gamma}$H), 4.81 (br s, 2H, C<u>H$_2$</u>OH), 4.73 (t, *J*= 8.4 Hz, 1H, Pro-$_{\alpha}$H), 4.65-4.60 (m, 1H, Pro-$_{\delta}$H), 4.21 (d, *J*= 9.6 Hz, 1H, Tle-$_{\alpha}$H), 4.07-4.02 (m, 1H, Pro-$_{\delta}$H), 3.77 (s, 3H, O-CH_3), 2.91-2.86 (m, 2H, Pro-$_{\beta}$H), 1.43 (s, 9H, ^{t}butyl), 1.04 (s, 9H, Tle–$_{\gamma}$H). ^{13}C NMR (101 MHz, $CDCl_3$) δ 171.2, 171.1, 156.2, 132.2, 128.6, 80.2, 58.8, 57.4, 56.3, 53.1, 52.6, 52.4, 35.7, 33.9, 28.5, 26.4. HRMS-ESI calculated for $C_{20}H_{33}N_5NaO_6$ [M+Na^+] 462.23230, found *m/z* 462.23112.

***tert*-Butyl N-[(2*S*)-1-[(2*S*,4*R*)-4-(4,5-dihydroxy-1H-1,2,3-triazol-1-yl)-2-{[1-(diphenoxyphosphoryl)-2-methylpropyl]carbamoyl}pyrrolidin-1-yl]-3,3-dimethyl-1-oxobutan-2-yl]carbamate (42).**

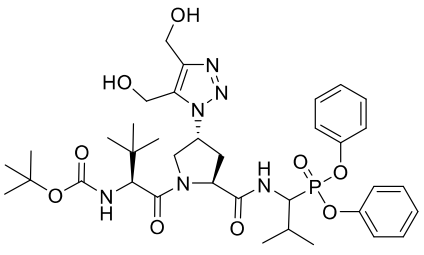

Compound **32** (64.0 mg, 0.136 mmol) and $LiOH.H_2O$ (29.0 mg, 0.682 mmol) in THF:H_2O (3:1 mL) were reacted and purified as described in Method D. The resulting acid compound (41.7 mg, 92.0 μmol), **18** (42.5 mg, 0.110 mmol), DIPEA (30 μL, 0.229 mmol), and HBTU (41.7 mg, 0.110 mmol) in DMF (2 mL) were reacted as described in Method A above. The crude product was purified by flash column chromatography with 1:4 to 0:100 PE:EtOAc, followed by 10% methanol in EtOAc to obtain a colourless oil as a mixture of two diastereomers (58 mg, 78.1

μmol, R_f 0.33, 0.26 in 100% EtOAc, 85%). $[\alpha]_{589}^{21}$= -0.52 (*c* = 0.5, $CHCl_3$). ^{1}H NMR (400 MHz, $CDCl_3$) δ 8.06 (d, *J*= 10.0 Hz, 0.5H, 0.5 × -NH), 7.67 (d, *J*= 10.4 Hz, 0.5H, 0.5 × -NH), 7.31-7.11 (m, 10 H, Phenoxy-H), 5.30 (d, *J*= 10.3 Hz, 0.5H, 0.5 × -NH), 5.20 (d, *J*= 9.9 Hz, 0.5H, 0.5 × -NH), 5.03-5.00 (m, 1H, Pro-$_\gamma$H), 4.88-4.66 (m, 6H, 1 × Val-$_\alpha$H, 1 × Pro-$_\alpha$H, 2 × C$\underline{H_2}$OH), 4.39-4.28 (m, 1H, Pro-$_\delta$H), 3.95-3.91 (m, 1H, Tle-$_\alpha$H), 3.85-3.81 (m, 1H, Pro-$_\delta$H), 3.64 (br. s, 2H, 2 × -OH), 3.05 (br. s, 1H, Pro-$_\beta$H), 2.81-2.78 (m, 0.5H, 0.5 × Pro-$_\beta$H), 2.66-2.62 (m, 0.5H, 0.5 × Pro-$_\beta$H), 2.48-2.40 (m, 1H, Val-$_\beta$H), 1.33 (s, 9H, ^{t}butyl), 1.19-1.15 (m, 3H, Val-$_\gamma$H), 1.09-1.07 (m, 3H, Val-$_\gamma$H), 0.92-0.83 (s, 9H, Tle–$_\gamma$H). ^{13}C NMR (101 MHz, $CDCl_3$) δ 172.2, 171.7, 171.2 (d, $J_{C\text{-}P}$= 5.8 Hz), 171.0 (d, $J_{C\text{-}P}$= 7.6 Hz), 155.99, 155.95, 150.5 (d, $J_{C\text{-}P}$= 9.7 Hz), 150.23 (d, $J_{C\text{-}P}$= 9.4 Hz), 150.19 (d, $J_{C\text{-}P}$= 9.6 Hz), 130.0, 129.91, 129.88, 120.8, 125.5 125.40, 125.37, 121.0 (d, $J_{C\text{-}P}$= 4.2 Hz), 120.8 (d, $J_{C\text{-}P}$= 4.1 Hz), 120.5 (d, $J_{C\text{-}P}$= 4.3 Hz), 80.3, 59.3, 59.2, 58.40, 58.36, 58.19, 58.18, 55.6, 54.6, 54.5, 52.11, 52.10, 51.8 (d, $J_{C\text{-}P}$= 154.5 Hz), 51.37 (d, $J_{C\text{-}P}$= 153.9 Hz), 35.7, 35.5, 33.1, 32.6, 29.44 (d, $J_{C\text{-}P}$= 4.2 Hz), 29.40 (d, $J_{C\text{-}P}$= 4.0 Hz), 28.4, 26.3, 26.2, 20.8 (d, $J_{C\text{-}P}$= 14.4 Hz), 20.5 (d, $J_{C\text{-}P}$= 13.9 Hz), 18.2 (d, $J_{C\text{-}P}$= 4.5 Hz), 18.1 (d, $J_{C\text{-}P}$= 4.3 Hz). ^{31}P NMR (162 MHz, $CDCl_3$) δ 17.51 (42.2%), 16.68 (57.6%). HRMS-ESI calculated for $C_{36}H_{51}N_6NaO_9P$ [M+Na^+] 765.33473, found *m/z* 765.33358. Analytical RP-HPLC (Table S9 for HPLC methods) t_R=16.31, 17.01 min.

tert-Butyl N-[(2*S*)-1-[(2*S*,4*S*)-4-(4,5-dihydroxy-1H-1,2,3-triazol-1-yl)-2-{[1-(diphenoxyphosphoryl)-2-methylpropyl]carbamoyl}pyrrolidin-1-yl]-3,3-dimethyl-1-oxobutan-2-yl]carbamate (43).

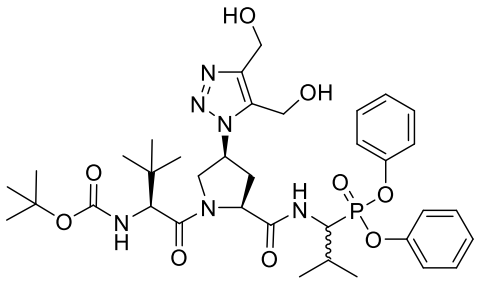

Compound **33** (71.0 mg, 0.151 mmol) and $LiOH.H_2O$ (31.7 mg, 0.756 mmol) in THF:H_2O (3:1 mL) were reacted and purified as described in Method D. The resulting acid compound (71.0 mg, 0.156 mmol), **18** (72.2 mg, 0.187 mmol), DIPEA (68 μL, 0.390 mmol), and HBTU (70.9 mg, 0.187 mmol) in DMF (2 mL) were reacted then the product purified as described in Method A. The product was isolated by flash column chromatography (10% methanol in EtOAc) to obtain an orange oil as a mixture of two diastereomers (42.1 mg, 56.7 μmol, R_f 0.14 in 1:1 n-Hex:EtOAc, 36%). $[\alpha]_{589}^{21}$= -11.64 (*c* = 0.5, $CHCl_3$). ^{1}H NMR (400 MHz, $CDCl_3$) δ 7.65 (d, *J*= 10.2 Hz, 0.5H, 0.5 × -NH), 7.58 (d, *J*= 10.5 Hz, 0.5H, 0.5 × -NH), 7.32-7.05 (m, 10 H, Phenoxy-H), 5.37 (d, *J*= 9.5 Hz, 0.5H,

0.5 × -NH), 5.30 (d, *J*= 9.5 Hz, 0.5H, 0.5 × -NH), 5.05-4.94 (m, 1H, Pro-$_{\gamma}$H), 4.78-4.59 (m, 6H, 1 × Val-$_{\alpha}$H, 1 × Pro-$_{\alpha}$H, 2 × C$\underline{H_2}$OH), 4.54-4.48 (m, 0.5H, 0.5 × Pro-$_{\delta}$H), 4.47-4.42 (m, 0.5H, 0.5 × Pro-$_{\delta}$H), 4.32-4.17 (m, 2H, 1 × Tle-$_{\alpha}$H, 1 × Pro-$_{\delta}$H), 3.23 (br. s, 2H, 2 × -OH), 2.92-2.70 (m, 2H, Pro-$_{\beta}$H), 2.41-2.36 (m, 1H, Val-$_{\beta}$H), 1.42 (s, 9H, ^{t}butyl), 1.14-1.10 (m, 3H, Val-$_{\gamma}$H), 1.07-0.92 (m, 12H, 3 × Val-$_{\gamma}$H, 9 × Tle–$_{\gamma}$H). ^{13}C NMR (101 MHz, $CDCl_3$) δ 172.9, 172.4, 170.7 (d, $J_{C\text{-}P}$= 5.5 Hz), 170.5 (d, $J_{C\text{-}P}$= 6.3 Hz), 156.2, 156.1, 150.5 (d, $J_{C\text{-}P}$= 9.8 Hz), 150.2 (d, $J_{C\text{-}P}$= 9.8 Hz), 150.1 (d, $J_{C\text{-}P}$= 9.3 Hz), 129.99, 129.96, 129.93, 129.88, 125.54, 125.50, 125.4, 121.0 (d, $J_{C\text{-}P}$= 4.1 Hz), 120.7 (d, $J_{C\text{-}P}$= 4.1 Hz), 120.4 (d, $J_{C\text{-}P}$= 4.1 Hz), 80.3, 80.2, 59.3, 59.1, 59.0, 58.9, 56.9, 56.7, 55.6, 52.1, 51.8 (d, $J_{C\text{-}P}$= 153.8 Hz), 51.4 (d, $J_{C\text{-}P}$= 154.7 Hz), 35.8, 35.3, 33.6, 33.3, 29.5 (d, $J_{C\text{-}P}$= 3.5 Hz), 28.52, 28.51, 26.5, 26.4, 20.7 (d, $J_{C\text{-}P}$= 13.8 Hz), 20.4 (d, $J_{C\text{-}P}$= 13.8 Hz), 18.2 (d, $J_{C\text{-}P}$= 4.6 Hz), 18.0 (d, $J_{C\text{-}P}$= 4.0 Hz). ^{31}P NMR (162 MHz, $CDCl_3$) δ 17.17 (23.2%), 16.93 (76.8%). HRMS-ESI calculated for $C_{36}H_{52}N_6O_9P$ [M+H$^+$] 743.35279, found *m/z* 743.35306. Analytical RP-HPLC (Table S9 for HPLC methods) t_R=16.09, 16.26 min.

tert-Butyl N-[(2*S*)-2-[(2*S*,4*R*)-2-{[1-(diphenoyphosphoryl)2-methylpropyl]carbamoyl}-4-[4-(2-hydroxypropan-2-yl)-1H-1,2,3-triazol-1-yl]pyrrolidin-1-yl]-3,3-dimethyl-1-oxobutan-2-yl]carbamate (44).

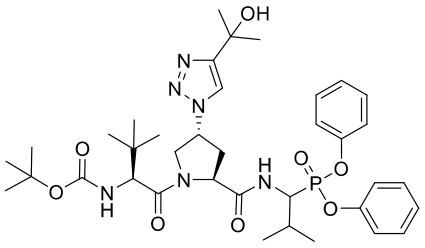

Compound **34** (67.0 mg, 0.143 mmol) and $LiOH.H_2O$ (30.0 mg, 0.716 mmol) in THF:H_2O (3:1 mL) were reacted and purified as described in Method D. The resulting acid compound (63.7 mg, 0.145 mmol), **18** (67.0 mg, 0.174 mmol), DIPEA (63 µL, 0.363 mmol), and HBTU (66.0 mg, 0.174 mmol) in DMF (2 mL) were reacted as described in Method A. The product was isolated by flash column chromatography with 1:1 to 100:0 EtOAc:n-Hex to obtain a colourless oil as a mixture of two diastereomers (40.0 mg, 54.0 µmol, R_f 0.14 in 1:1 n-Hex:EtOAc, 37 %). $[\boldsymbol{\alpha}]_{589}^{21}$= 3.44 (*c* = 0.5, $CHCl_3$). ^{1}H NMR (400 MHz, $CDCl_3$) δ 7.67 (br s, 1H, triazolyl-H), 7.46 (d, *J*= 10.2 Hz, 1H, -NH), 7.32-7.11 (m, 10H, Phenoxy-H), 5.35-5.28 (m, 1H, Pro-$_{\gamma}$H), 5.23 (d, *J*= 9.0 Hz, 0.5H, 0.5 × -NH), 5.16 (d, *J*= 9.4 Hz, 0.5H, 0.5 × -NH), 4.94 (br. s, 0.5H, 0.5 × Pro-$_{\alpha}$H), 4.79-4.71 (m, 1H, Val-$_{\alpha}$H), 4.65 (br. s, 0.5H, 0.5 × Pro-$_{\alpha}$H), 4.26-4.08 (m, 3H, 2 × Pro-$_{\delta}$H, 1 × Tle-$_{\alpha}$H), 2.94-2.90 (m, 0.5H, 0.5 × Pro-$_{\beta}$H), 2.65 (br. s, 1H, Pro-$_{\beta}$H), 2.50-2.39 (m, 2.5H, 1 × -OH, 1 × Val-$_{\beta}$H, 0.5 × Pro-$_{\beta}$H), 1.62 (br. s, 6H, C(C$\underline{H_3}$)$_{\underline{2}}$,OH), 1.40 (m, 9H, ^{t}butyl), 1.15-1.13 (m, 3H, Val-$_{\gamma}$H), 1.09-1.05 (m, 3H, Val-$_{\gamma}$H), 1.01 (s, 4.5H, Tle–$_{\gamma}$H), 1.92 (s, 4.5H,

Tle–$_{\gamma}$H). ^{13}C NMR (101 MHz, $CDCl_3$) δ 172.4, 171.8, 170.7 (d, $J_{C\text{-}P}$= 7.1 Hz), 170.5 (d, $J_{C\text{-}P}$= 5.6 Hz), 155.84, 155.83, 150.4 (d, $J_{C\text{-}P}$= 9.9 Hz), 150.1 (d, $J_{C\text{-}P}$= 10.4 Hz), 150.0 (d, $J_{C\text{-}P}$= 9.1 Hz), 129.8 (d, $J_{C\text{-}P}$= 0.7 Hz), 129.74, 129.73, 129.7 (d, $J_{C\text{-}P}$= 0.8 Hz), 125.4 (d, $J_{C\text{-}P}$= 1.0 Hz), 125.34 (d, $J_{C\text{-}P}$= 1.1 Hz), 125.26 (d, $J_{C\text{-}P}$= 1.1 Hz), 125.2, 120.8 (d, $J_{C\text{-}P}$= 4.0 Hz), 120.7 (d, $J_{C\text{-}P}$= 4.4 Hz), 120.5 (d, $J_{C\text{-}P}$= 4.2 Hz), 120.3 (d, $J_{C\text{-}P}$= 4.2 Hz), 80.1, 80.0, 68.44, 68.38, 59.91, 58.98, 58.95, 58.90, 58.80, 53.00, 52.97, 51.6 (d, $J_{C\text{-}P}$= 154.6 Hz), 51.2 (d, $J_{C\text{-}P}$= 154.2 Hz), 35.4, 35.1, 34.1, 34.0, 30.5, 30.4, 29.27, 29.23, 28.3, 26.4, 26.2, 20.6 (d, $J_{C\text{-}P}$= 13.6 Hz), 20.3 (d, $J_{C\text{-}P}$= 13.6 Hz), 18.0 (d, $J_{C\text{-}P}$= 4.0 Hz), 17.9 (d, $J_{C\text{-}P}$= 4.0 Hz). ^{31}P NMR (162 MHz, $CDCl_3$) δ 16.96 (28.4%), 16.38 (71.6%). HRMS-ESI calculated for $C_{37}H_{53}N_6NaO_8P$ [M+H$^+$] 763.35547, found *m/z* 763.35248. Analytical RP-HPLC (Table S9 for HPLC methods) t_R=21.09, 21.62 min.

***tert*-Butyl N-[(2S)-1-[(2*S*,4*R*)-2-{[1-(diphenoxyphosphoryl)-2-methylpropyl]carbamoyl}-4-[4-(hydroxymethyl)-1H-1,2,3-triazol-1-yl]pyrrolidin-1-yl]-3,3-dimethyl-1-oxobutan-2-yl]carbamate (45).**

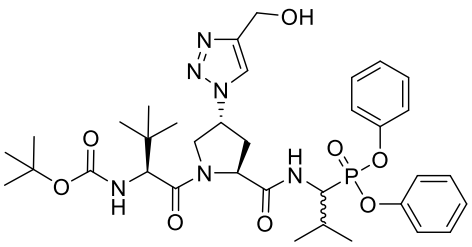

Compound **35** (35.0 mg, 79.6 μmol) and $LiOH.H_2O$ (16.7 mg, 0.398 mmol) in THF:H_2O (3:1 mL) were reacted and purified as described in Method D. The resulting acid compound (31.0 mg, 72.9 μmol), **18** (33.8 mg, 87.4 μmol), DIPEA (32 μL, 0.182 mmol), and HBTU (40.0 mg, 87.4 μmol) in DMF (2 mL) were reacted as described in Method A. The product was isolated by flash column chromatography with 1:1 to 0:100 EtOAc:n-Hex to obtain a colourless oil as a mixture of two diastereomers (15.0 mg, 3.16 μmol, R_f 0.13 in 100% EtOAc, 43%). $[\boldsymbol{\alpha}]_{589}^{21}$= -19.32 (*c* = 0.5, $CHCl_3$). ^{1}H NMR (400 MHz, $CDCl_3$) δ 8.09 (d, *J*= 10.2 Hz, 0.5H, 0.5 × -NH), 7.79 (s, 1H, triazolyl-H), 7.51 (d, *J*= 10.4 Hz, 0.5H, 0.5 × -NH), 7.31-7.10 (m, 10H, Phenoxy-H), 5.29 (br. s, 1H, Pro-$_{\gamma}$H), 5.25 (d, *J*= 8.8 Hz, 0.5H, 0.5 × -NH), 5.18 (d, *J*= 9.4 Hz, 0.5H, 0.5 × -NH), 4.86-4.62 (m, 4H, 1 × Pro-$_{\alpha}$H, 1 × Val-$_{\alpha}$H, C$\underline{H_2}$OH), 4.43-4.36 (m, 1H, Pro-$_{\delta}$H), 4.17-4.05 (m, 2H, 1 × Pro-$_{\delta}$H, 1 × Tle-$_{\alpha}$H), 2.81-2.78 (m, 1H, Pro-$_{\beta}$H), 2.64-2.52 (m, 2H, 1 × Pro-$_{\beta}$H, 1 × -OH), 2.47-2.39 (m, 1H, Val-$_{\beta}$H), 1.39 (s, 9H, ^{t}butyl), 1.15-1.05 (m, 6H, Val-$_{\gamma}$H), 1.02-0.96 (s, 9H, Tle–$_{\gamma}$H). ^{13}C NMR (101 MHz, $CDCl_3$) δ 172.4, 172.1, 171.0 (d, $J_{C\text{-}P}$= 5.7 Hz), 170.9 (d, $J_{C\text{-}P}$= 5.9 Hz), 156.2, 150.6 (d, $J_{C\text{-}P}$= 10.1 Hz), 150.22 (d, $J_{C\text{-}P}$= 9.5 Hz), 150.21 (d, $J_{C\text{-}P}$= 9.5 Hz), 130.0 (d, $J_{C\text{-}P}$= 0.7 Hz), 129.9 (d, $J_{C\text{-}P}$= 1.0 Hz), 129.8 (d, $J_{C\text{-}P}$=

0.4 Hz), 125.50 (d, $J_{C\text{-}P}$= 0.7 Hz), 125.46 (d, $J_{C\text{-}P}$= 1.0 Hz), 125.4, 125.3, 121.1 (d, $J_{C\text{-}P}$= 4.1 Hz), 121.0 (d, $J_{C\text{-}P}$= 4.3 Hz), 120.7 (d, $J_{C\text{-}P}$= 4.2 Hz), 120.5 (d, $J_{C\text{-}P}$= 4.3 Hz), 80.28, 80.26, 59.38, 59.35, 59.1, 58.9, 58.8, 56.3, 56.1, 53.2, 53.1, 51.8 (d, $J_{C\text{-}P}$= 155.4 Hz), 51.2 (d, $J_{C\text{-}P}$= 155.2 Hz), 35.3, 35.12, 35.08, 34.7, 29.48, 29.45, 28.5, 26.5, 26.4, 20.7 (d, $J_{C\text{-}P}$= 14.2 Hz), 20.5 (d, $J_{C\text{-}P}$= 13.7 Hz), 18.14 (d, $J_{C\text{-}P}$= 6.0 Hz), 18.09 (d, $J_{C\text{-}P}$= 4.1 Hz). ^{31}P NMR (162 MHz, $CDCl_3$) δ 17.27 (37.5%), 16.54 (62.5%). HRMS-ESI calculated for $C_{35}H_{49}N_6NaO_8P$ [M+H$^+$] 735.32417, found *m/z* 735.32129. Analytical RP-HPLC (Table S9 for HPLC methods) t_R=18.36, 19.03 min.

***tert*-Butyl N-[(2*S*)-1-[(2*S*,4*S*)-2-{[1-(diphenoxyphosphoryl)-2-methylpropyl]carbamoyl}-4-[4-(hydroxymethyl)-1H-1,2,3-triazol-1-yl]pyrrolidin-1-yl]-3,3-dimethyl-1-oxobutan-2-yl]carbamate (46).**

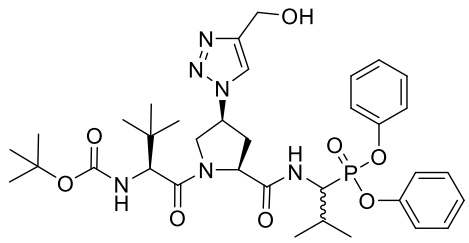

Compound **36** (53.0 mg, 0.121 μmol) and $LiOH.H_2O$ (25.3 mg, 0.603 mmol) in THF:H_2O (3:1 mL) were reacted and purified as described in Method D. The resulting acid compound (57.6 mg, 0.135 mmol), **18** (62.6 mg, 0.162 mmol), DIPEA (60 μL, 0.338 mmol), and HBTU (61.4 mg, 0.162 mmol) in DMF (2 mL) were reacted then purified as described in Method A. The product was isolated by flash column chromatography with 1:1 to 0:100 EtOAc:n-Hex to obtain a colourless oil as a mixture of two diastereomers (15.0 mg, 3.16 μmol, R_f 0.13 in 100% EtOAc, 43 %). $[\boldsymbol{\alpha}]_{589}^{21}$= -31.28 (*c* = 0.5, $CHCl_3$). ^{1}H NMR (400 MHz, $CDCl_3$) δ 7.72 (br s, 1H, triazolyl-H), 7.66 (d, *J*= 10.1 Hz, 0.5H, 0.5 × -NH), 7.49 (d, *J*= 10.4 Hz, 0.5H, 0.5 × -NH), 7.31-7.05 (m, 10H, Phenoxy-H), 5.40 (d, *J*= 9.3 Hz, 0.5H, 0.5 × -NH), 5.27 (d, *J*= 9.5 Hz, 0.5H, 0.5 × -NH), 5.19-5.15 (m, 0.5H, 0.5 × Pro-$_\gamma$H), 5.02-4.98 (m, 0.5H, 0.5 × Pro-$_\gamma$H), 4.90-4.86 (m, 0.5H, 0.5 × Pro-$_\alpha$H), 4.78-4.54 (m, 4.5H, 0.5 × Pro-$_\alpha$H, C$\underline{H_2}$OH, 1 × Val-$_\alpha$H, 1 × Pro-$_\delta$H), 4.28-4.24 (m, 1H, Tle-$_\alpha$H), 4.08-3.96 (m, 1H, Pro-$_\delta$H), 2.72-2.65 (m, 2H, 1 × Pro-$_\beta$H, 1 × -OH), 2.49-2.25 (m, 1H, Pro-$_\beta$H), 2.42-2.38 (m, 1H, Val-$_\beta$H), 1.42 (s, 9H, ^{t}butyl), 1.13-0.9 (m, 15H, 6 × Val-$_\gamma$H, 9 × Tle–$_\gamma$H). ^{13}C NMR (101 MHz, $CDCl_3$) δ 173.5, 172.0, 170.7 (d, $J_{C\text{-}P}$= 7.4 Hz), 170.5 (d, $J_{C\text{-}P}$= 6.4 Hz), 155.9, 155.8, 150.4 (d, $J_{C\text{-}P}$= 9.8 Hz), 150.0 (d, $J_{C\text{-}P}$= 9.9 Hz), 149.9 (d, $J_{C\text{-}P}$= 10.0 Hz), 129.9, 129.8 (d, $J_{C\text{-}P}$= 0.7 Hz), 129.8, 125.4, 125.2, 120.7 (d, $J_{C\text{-}P}$= 4.2 Hz), 120.5 (d, $J_{C\text{-}P}$= 4.2 Hz), 120.2 (d, $J_{C\text{-}P}$= 4.4 Hz), 80.1, 79.9, 59.4, 58.9, 58.7, 58.3, 57.8, 56.5, 56.4, 53.4, 52.8, 51.6 (d, $J_{C\text{-}P}$= 155.3 Hz), 51.3 (d, $J_{C\text{-}P}$= 155.8 Hz), 35.7, 35.1, 33.5,

33.4, 29.33 (d, $J_{C\text{-}P}$= 3.4 Hz), 29.28 (d, $J_{C\text{-}P}$= 3.3 Hz), 28.4, 28.3, 26.3, 26.2, 20.6 (d, $J_{C\text{-}P}$= 13.9 Hz), 20.3 (d, $J_{C\text{-}P}$= 14.4 Hz), 18.0 (d, $J_{C\text{-}P}$= 4.5 Hz), 17.9 (d, $J_{C\text{-}P}$= 3.7 Hz). ^{31}P NMR (162 MHz, $CDCl_3$) δ 16.85 (39.7%), 16.56 (60.3%). HRMS-ESI calculated for $C_{35}H_{49}N_6NaO_8P$ [M+H$^+$] 735.32417, found *m/z* 735.32183. Analytical RP-HPLC (Table S9 for HPLC methods) t_R=17.75 min.

***tert*-Butyl N-[(2*S*)-1-[(2*S*,4*R*)-4-(4-carbamoyl-1H-1,2,3-triazol-1-yl)-2-{[1-(diphenoxyphosphoryl)-2-methylpropyl]carbamoyl}pyrrolidin-1-yl]-3,3-dimethyl-1-oxobutan-2-yl]carbamate (47).**

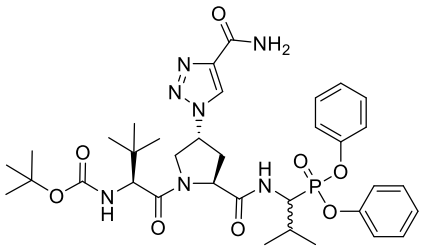

Compound **37** (25.0 mg, 55.2 μmol) and $LiOH.H_2O$ (11.6 mg, 0.276 mmol) in THF:H_2O (3:1 mL) were reacted and purified as described in Method D. The resulting acid compound (26.0 mg, 59.3 μmol), **18** (27.5 mg, 71.2 μmol), DIPEA (20 μL, 88.9 μmol), and HBTU (27.0 mg, 71.2 μmol) in DMF (2 mL) were reacted as described in Method A. The crude was further purified by flash column chromatography with 1:4 to 0:100 n-Hex:EtOAc, followed by 10% methanol in EtOAc to obtain a colourless oil as a mixture of two diastereomers (29.0 mg, 40.0 μmol, R_f 0.30 in 100% EtOAc, 67%). $[\boldsymbol{\alpha}]_{589}^{21}$= -14.88 (*c* = 0.5, $CHCl_3$). ^{1}H NMR (400 MHz, $CDCl_3$) δ 8.36 (s, 0.5H, 0.5 × triazolyl-H), 8.25 (s, 0.5H, 0.5 × triazolyl-H), 7.84 (d, *J*= 10.3 Hz, 0.5H, 0.5 × -NH), 7.32-7.09 (m, 10H, Phenoxy-H), 6.99 (d, *J*= 8.8 Hz, 0.5H, 0.5 × -NH), 6.69 (s, 1H, triazolyl-CONH), 6.49 (s, 1H, triazolyl-CONH), 5.37-5.32 (m, 1H, Pro-$_\gamma$H), 5.25 (d, *J*= 9.1 Hz, 0.5H, 0.5 × -NH), 5.17 (d, *J*= 9.5 Hz, 0.5H, 0.5 × -NH), 5.04-5.01 (m, 0.5H, 0.5 × Pro-$_\alpha$H), 4.88-4.74 (m, 1.5H, 0.5 × Pro-$_\alpha$H, 1 × Val-$_\alpha$H), 4.38-4.32 (m, 1H, Pro-$_\delta$H), 4.20-4.13 (m, 2H, 1 × Pro-$_\delta$H, 1 × Tle-$_\alpha$H), 2.95-2.89 (m, 0.5H, 0.5 × Pro-$_\beta$H), 2.80-2.73 (m, 0.5H, 0.5 × Pro-$_\beta$H), 2.49-2.34 (2H, 1 × Pro-$_\beta$H, 1 × Val-$_\beta$H), 1.35 (s, 9H, ^{t}butyl), 1.17-1.05 (m, 6H, Val-$_\gamma$H), 1.00-0.92 (s, 9H, Tle–$_\gamma$H). ^{13}C NMR (101 MHz, $CDCl_3$) δ 172.6, 171.8, 171.1 (d, $J_{C\text{-}P}$= 5.9 Hz), 171.0 (d, $J_{C\text{-}P}$= 5.8 Hz), 162.2, 162.1, 155.92, 155.85, 150.7 (d, $J_{C\text{-}P}$= 9.6 Hz), 150.22 (d, $J_{C\text{-}P}$= 10.1 Hz), 150.16 (d, $J_{C\text{-}P}$= 9.6 Hz), 143.1, 143.0, 130.0, 129.94 (d, $J_{C\text{-}P}$= 0.6 Hz), 129.86, 129.8 (d, $J_{C\text{-}P}$= 0.6 Hz), 125.6, 125.54 (d, $J_{C\text{-}P}$= 1.0 Hz), 125.49 (d, $J_{C\text{-}P}$= 1.0 Hz), 125.4 (d, $J_{C\text{-}P}$= 0.6 Hz), 125.3, 124.8, 120.92 (d, $J_{C\text{-}P}$= 4.2 Hz), 120.90 (d, $J_{C\text{-}P}$= 4.1 Hz), 120.6 (d, $J_{C\text{-}P}$= 4.2 Hz), 120.4 (d, $J_{C\text{-}P}$= 4.2 Hz), 80.1, 80.0, 59.7, 59.2, 59.0, 58.9, 58.8, 53.7, 53.3, 51.7 (d, $J_{C\text{-}P}$= 155.5 Hz), 51.3 (d, $J_{C\text{-}P}$= 155.5 Hz), 35.5, 35.2, 34.0, 29.44 (d, $J_{C\text{-}P}$= 3.8 Hz), 29.39 (d, $J_{C\text{-}P}$= 3.9 Hz),

28.4, 26.4, 26.3, 20.8 (d, $J_{C\text{-}P}$= 14.2 Hz), 20.4 (d, $J_{C\text{-}P}$= 14.4 Hz), 18.0 (d, $J_{C\text{-}P}$= 3.5 Hz), 17.9 (d, $J_{C\text{-}P}$= 3.2 Hz). ^{31}P NMR (162 MHz, $CDCl_3$) δ 17.13 (43.8%), 16.91 (56.2%). HRMS-ESI calculated for $C_{35}H_{48}N_7NaO_8P$ [M+H$^+$] 748.31942, found *m/z* 748.31843. Analytical RP-HPLC (Table S9 for HPLC methods) t_R=19.13, 19.96 min

***tert*-Butyl N-[(2*S*)-1-[(2*S*,4*R*)-2-{[1-(diphenoxyphosphoryl)-2-methylpropyl]carbamoyl}-4-[5-(2-hydroxypropan-2-yl)-1H-1,2,3-triazol-1-yl]pyrrolidin-1-yl]-3,3-dimethyl-1-oxobutan-2-yl]carbamate (48).**

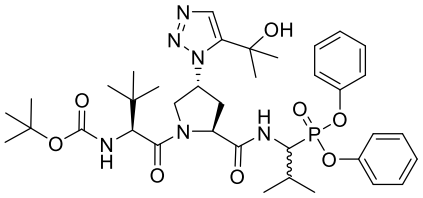

Compound **38** (0.11 g, 0.227 mmol), $LiOH.H_2O$ (47.6 mg, 1.13 mmol) in THF:H_2O (3:1 mL) were reacted and purified as described in Method D. The resulting acid compound (61.6 mg, 0.140 mmol), **18** (65.3 mg, 0.169 mmol), DIPEA (61 µL, 0.350 mmol), and HBTU (64.1 mg, 0.169 mmol) in DMF (2 mL) were reacted as described in Method A. The crude was further purified by flash column chromatography with 2:3 to 0:100 n-Hex:EtOAc to obtain a colourless oil as a mixture of two diastereomers (33.3 mg, 44.9 µmol, R_f 0.31, 0.38 in 3:7 n-Hex:EtOAc, 32%). $[\alpha]_{589}^{21}$= -28.40 (*c* = 0.5, $CHCl_3$). ^{1}H NMR (400 MHz, $CDCl_3$) δ 7.88 (d, *J*= 10.2 Hz, 0.5H, 0.5 × -NH), 7.72 (d, *J*= 10.0 Hz, 0.5H, 0.5 × -NH), 7.49 (br s, 1H, triazolyl-H), 7.31-7.10 (m, 10 H, Phenoxy-H), 5.74-5.69 (m, 1H, Pro-$_\gamma$H), 5.30 (d, *J*= 9.6, 0.5H, 0.5 × -NH), 5.20 (d, *J*= 10.1 Hz, 0.5H, 0.5 × -NH), 5.11-5.07 (m, 0.5H, 0.5 × Pro-$_\alpha$H), 4.83-4.71 (m, 1.5H, 0.5 × Pro-$_\alpha$H, 1 × Val-$_\alpha$H), 4.37-4.34 (m, 0.5H, 0.5 × Pro-$_\delta$H), 4.25-4.22 (m, 0.5H, 0.5 × Pro-$_\delta$H), 4.03-3.92 (m, 2H, 1 × Pro-$_\delta$H, 1 × Tle-$_\alpha$H), 2.95-2.92 (m, 0.5H, 0.5 × Pro-$_\beta$H), 2.83-2.81 (m, 0.5H, 0.5 × Pro-$_\beta$H), 2.73-2.769 (m, 0.5H, 0.5 × Pro-$_\beta$H), 2.58-2.3.51 (m, 0.5H, 0.5 × Pro-$_\beta$H), 2.48-2.41 (m, 1H, Val-$_\beta$H), 1.68 (s, 3H, C(C$\underline{H_3}$)$_2$OH), 1.60 (s, 3H, C(C$\underline{H_3}$)$_2$OH), 1.32 (s, 9H, ^{t}butyl), 1.20-1.16 (m, 3H, Val-$_\gamma$H), 1.11-1.06 (m, 3H, Val-$_\gamma$H), 0.94 (s, 4.5H, Tle–$_\gamma$H), 0.83 (s, 4.5H, Tle–$_\gamma$H). ^{13}C NMR (101 MHz, $CDCl_3$) δ 172.0, 171.3, 171.32 (d, $J_{C\text{-}P}$= 6.3 Hz), 171.2 (d, $J_{C\text{-}P}$= 5.6 Hz), 155.8, 155.7, 150.5 (d, $J_{C\text{-}P}$= 9.8 Hz), 150.3 (d, $J_{C\text{-}P}$= 9.2 Hz), 150.2 (d, $J_{C\text{-}P}$= 9.6 Hz), 132.3, 132.18, 132.16, 132.1, 129.9 (d, $J_{C\text{-}P}$= 0.9 Hz), 129.83, 129.78 (d, $J_{C\text{-}P}$= 0.6 Hz), 128.7, 128.6, 125.4, 125.3, 121.1 (d, $J_{C\text{-}P}$= 3.9 Hz), 120.93 (d, $J_{C\text{-}P}$= 4.5 Hz), 120.85 (d, $J_{C\text{-}P}$= 4.2 Hz), 120.6 (d, $J_{C\text{-}P}$= 4.5 Hz), 80.1, 80.0, 67.2, 67.0, 59.6, 59.5, 58.64, 58.55, 58.2, 54.63, 54.56, 51.7 (d, $J_{C\text{-}P}$= 153.6 Hz), 51.3 (d, $J_{C\text{-}P}$= 154.4 Hz), 35.9, 35.6, 33.9, 33.8, 31.02, 30.97, 29.5 (d, $J_{C\text{-}P}$= 4.7 Hz), 29.4 (d, $J_{C\text{-}P}$= 4.6 Hz), 28.4, 26.3, 26.2, 20.8 (d, $J_{C\text{-}P}$= 13.8 Hz), 20.6 (d, $J_{C\text{-}P}$= 13.8 Hz), 18.3 (d, $J_{C\text{-}P}$= 4.6 Hz),

18.1 (d, $J_{C\text{-}P}$= 4.3 Hz). ^{31}P NMR (162 MHz, $CDCl_3$) δ 17.56 (49.6%), 16.95 (50.4%). HRMS-ESI calculated for $C_{37}H_{53}N_6NaO_8P$ [M+H$^+$] 763.35547, found *m/z* 763.35427. Analytical RP-HPLC (Table S9 for HPLC methods) t_R=23.92, 24.21 min.

***tert*-Butyl N-[(2*S*)-1-[(2*S*,4*S*)-2-{[1-(diphenoxyphosphoryl)-2-methylpropyl]carbamoyl}-4-[5-(2-hydroxypropan-2-yl)-1H-1,2,3-triazol-1-yl]pyrrolidin-1-yl]-3,3-dimethyl-1-oxobutan-2-yl]carbamate (49).**

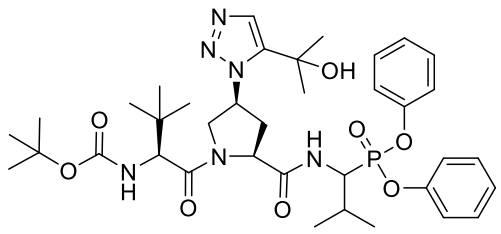

Compound **39** (67.2 mg, 0.144 mmol) and $LiOH.H_2O$ (30.2 mg, 0.719 mmol) in THF:H_2O (3:1 mL) were reacted and purified as described in Method D. The resulting acid compound (64.0 mg, 0.146 mmol), **18** (67.7 mg, 0.175 mmol), DIPEA (64 µL, 0.365 mmol), and HBTU (66.4 mg, 0.175 mmol) in DMF (2 mL) were reacted following Method A. The crude was further purified by flash column chromatography with 2:3 to 0:100 n-Hex:EtOAc to obtain a colourless oil as a mixture of two diastereomers (61.0 mg, 82.3 µmol, 56%). $[\alpha]_{589}^{21}$= -10.40 (*c* = 0.5, $CHCl_3$). ^{1}H NMR (400 MHz, $CDCl_3$) δ 7.64 (d, *J*= 9.8 Hz, 0.5H, 0.5 × -NH), 7.47 (d, *J*= 9.8 Hz, 0.5H, 0.5 × -NH), 7.43-7.42 (m, 1H, triazolyl-H), 7.30-7.04 (m, 10 H, Phenoxy-H), 5.54 (br s, 1H, Pro-$_\gamma$H), 5.37 (d, *J*= 9.5 Hz, 0.5H, 0.5 × -NH), 5.30 (d, *J*= 9.5 Hz, 0.5H, 0.5 × -NH), 4.83-4.71 (m, 1.5H, 1 × Val-$_\alpha$H, 0.5 × Pro-$_\alpha$H), 4.61-4.47 (m, 1.5H, 0.5 × Pro-$_\alpha$H, 1 × Pro-$_\delta$H), 4.27-4.22 (m, 1H, Tle-$_\alpha$H), 4.19-4.14 (m, 0.5H, 0.5 × Pro-$_\delta$H), 4.06-4.01 (m, 0.5H, 0.5 × Pro-$_\delta$H), 3.06-3.00 (m, 2H, 1 × Pro-$_\beta$H, 1 × -OH), 2.92-2.87 (m, 1H, Pro-$_\beta$H), 2.43-2.37 (m, 1H, Val-$_\beta$H), 1.64-1.61 (m, 6H, C(C$\underline{H_3}$)$_2$,OH), 1.404-1.397 (m, 9H, ^{t}butyl), 1.14-1.04 (m, 6H, Val-$_\gamma$H), 1.00-0.84 (s, 9H, Tle-$_\gamma$H). ^{13}C NMR (101 MHz, $CDCl_3$) δ 172.8, 172.3, 170.8 (d, $J_{C\text{-}P}$= 6.8 Hz), 170.6 (d, $J_{C\text{-}P}$= 6.7 Hz), 156.1, 150.5 (d, $J_{C\text{-}P}$= 9.9 Hz), 150.2 (d, $J_{C\text{-}P}$= 9.7 Hz), 150.1, 130.0 (d, $J_{C\text{-}P}$= 0.6 Hz), 129.91, 129.88 (d, $J_{C\text{-}P}$= 0.5 Hz), 125.50, 125.47, 125.3, 121.1 (d, $J_{C\text{-}P}$= 4.2 Hz), 121.0 (d, $J_{C\text{-}P}$= 4.1 Hz), 120.8 (d, $J_{C\text{-}P}$= 4.1 Hz), 120.5 (d, $J_{C\text{-}P}$= 4.3 Hz), 80.2, 80.1, 67.6, 59.24, 59.17, 58.93, 58.85, 57.3, 57.0, 53.4, 53.3, 51.6 (d, $J_{C\text{-}P}$= 154.4 Hz), 51.3 (d, $J_{C\text{-}P}$= 154.7 Hz), 35.7, 35.4, 34.2, 34.0, 30.83, 30.82, 30.7, 29.5 (d, $J_{C\text{-}P}$= 3.4 Hz), 28.48, 28.47, 26.43, 26.36, 20.7 (d, $J_{C\text{-}P}$= 13.4 Hz), 20.4 (d, $J_{C\text{-}P}$= 13.8 Hz), 18.21 (d, $J_{C\text{-}P}$= 4.2 Hz), 18.17 (d, $J_{C\text{-}P}$= 3.7 Hz). HRMS-ESI calculated for $C_{37}H_{53}N_6NaO_8P$ [M+H$^+$] 763.35547, found *m/z* 763.35505. Analytical RP-HPLC (Table S9 for HPLC methods) t_R=23.03, 23.62 min.

***tert*-Butyl N-[(2*S*)-1-[(2*S*,4*R*)-4-(5-carbamoyl-1H-1,2,3-triazol-1-yl)-2-{[1-(diphenoxyphosphoryl)-2-methylpropyl]carbamoyl}pyrrolidin-1-yl]-3,3-dimethyl-1-oxobutan-2-yl]carbamate (50).**

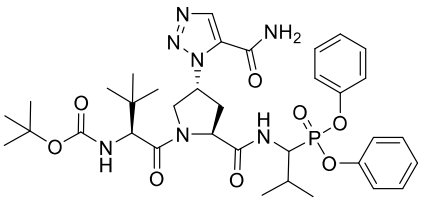

Compound **40** (26.0 mg, 57.5 μmol), LiOH.H_2O (12.1 mg, 0.287 mmol) in THF:H_2O (3:1 mL) were reacted and purified as described in Method D. The resulting acid compound (22.0 mg, 50.2 μmol), **18** (23.3 mg, 60.2 μmol), DIPEA (50 μL, 0.287 mmol), and HBTU (22.8 mg, 60.2 μmol) in DMF (2 mL) were reacted according to Method A. The crude was further purified by flash column chromatography with 2:3 to 0:100 n-Hex:EtOAc to obtain a colourless oil as a mixture of two diastereomers (11 mg, 15.2 μmol, 30%). $[\boldsymbol{\alpha}]_{589}^{21}$= -14.96 (*c* = 0.5, $CHCl_3$). ^{1}H NMR (400 MHz, $CDCl_3$) δ 8.34 (s, 0.5H, 0.5 × triazolyl-H), 8.25 (s, 0.5H, 0.5 × triazolyl-H), 7.76 (d, *J*= 9.9 Hz, 0.5H, 0.5 × -NH), 7.71 (d, *J*= 10.4 Hz, 0.5H, 0.5 × -NH), 7.33-7.09 (m, 10H, Phenoxy-H), 6.51 (s, 1H, triazolyl-CONH), 6.32 (s, 1H, triazolyl-CONH), 5.38-5.33 (m, 1H, Pro-$_\gamma$H), 5.22 (d, *J*= 9.4 Hz, 0.5H, 0.5 × -NH), 5.15 (d, *J*= 9.3 Hz, 0.5H, 0.5 × -NH), 5.02 (br. s, 0.5H, 0.5 × Pro-$_\alpha$H), 4.85-4.73 (m, 1.5H, 0.5 × Pro-$_\alpha$H, 1 × Val-$_\alpha$H), 4.37-4.34 (m, 1H, Pro-$_\delta$H), 4.22-4.12 (m, 2H, 1 × Pro-$_\delta$H, 1 × Tle-$_\alpha$H), 2.95-2.87 (m, 1H, Pro-$_\beta$H), 2.75 (br. s, 0.5H, 0.5 × Pro-$_\beta$H), 2.47-2.41 (m, 1.5H, 0.5 × Pro-$_\beta$H, 1 × Val-$_\beta$H), 1.36 (s, 9H, ^{t}butyl), 1.17-1.06 (m, 6H, Val-$_\gamma$H), 1.00 (s, 4.5H, Tle–$_\gamma$H), 0.92 (s, 4.5H, Tle–$_\gamma$H). ^{13}C NMR (101 MHz, $CDCl_3$) δ 172.6, 171.7, 170.8 (d, $J_{C\text{-}P}$= 7.1 Hz), 170.7 (d, $J_{C\text{-}P}$= 5.8 Hz), 162.0, 161.9, 155.8, 155.7, 150.6 (d, $J_{C\text{-}P}$= 9.8 Hz), 150.1 (d, $J_{C\text{-}P}$= 9.8 Hz), 150.0 (d, $J_{C\text{-}P}$= 9.5 Hz), 142.8, 129.9, 129.8, 129.72, 129.66, 125.43, 125.39, 125.3, 125.2, 124.7, 120.8 (d, $J_{C\text{-}P}$= 4.1 Hz), 120.7 (d, $J_{C\text{-}P}$= 4.3 Hz), 120.5 (d, $J_{C\text{-}P}$= 4.2 Hz), 120.2 (d, $J_{C\text{-}P}$= 4.2 Hz), 80.0, 79.9, 59.6, 59.1, 58.9, 58.8, 58.7, 53.5, 53.1, 51.5 (d, $J_{C\text{-}P}$= 155.7 Hz), 51.2 (d, $J_{C\text{-}P}$= 155.4 Hz), 35.3, 35.0, 33.8, 33.7, 29.3 (d, $J_{C\text{-}P}$= 3.5 Hz), 29.2 (d, $J_{C\text{-}P}$= 3.8 Hz), 28.2, 26.3, 26.2, 20.6 (d, $J_{C\text{-}P}$= 14.0 Hz), 20.3 (d, $J_{C\text{-}P}$= 14.4 Hz), 17.84 (d, $J_{C\text{-}P}$= 3.3 Hz), 17.80 (d, $J_{C\text{-}P}$= 4.6 Hz). ^{31}P NMR (162 MHz, $CDCl_3$) δ 17.09 (43.3%), 16.79 (56.7%). HRMS-ESI calculated for $C_{35}H_{48}N_7NaO_8P$ [M+H^+] 748.31942, found *m/z* 748.31705. Analytical RP-HPLC (Table S9 for HPLC methods) t_R=19.14, 19.97 min.

4.3. Homology modelling

Protein sequence for CtHtrA (Uniprot ID: P18584) was obtained from the UniProt database [61]. Sequence alignment was conducted using T-coffee server [62] and manually optimized where loops were missing from the template structure. Twenty homology models of CtHtrA were generated by Modeller® (version 9.19) using the crystal structure of DegP (HtrA in *E.coli*; PDB ID: 3MH6 [53]) as a template. The models were then evaluated by the DOPE (discrete optimised protein energy) score, which is the most reliable method for detecting native-like models [63]. The model with the best energy profile (most negative DOPE score) was then selected for CtHtrA.

4.4. Docking studies

Docking was conducted using Gold v5.2 with the homology model of CtHtrA. The ligands with pre-determined proline ring puckering were drawn by Avogadro an open-source molecular builder and visualization tool (version 1.2.0, http://avogadro.cc/ [64]). The ligands were then covalently docked based on mechanisms described by previous X-ray crystal structures of peptidic inhibitors covalently bound to serine proteases. The covalent binding between the phosphorus atom of the warhead and catalytic Ser247 hydroxyl oxygen was defined as the covalent linkage. Two key hydrogen bond constraints between the enzyme and ligands were pre-defined between NH of P1 amide and C=O of Thr263 and C=O of P3 backbone and NH of Ile265 amide. These hydrogen bond constraints were determined based on the crystal structure PDB 1EAT [65], and corresponded to those made when peptide-based ligands were docked. The docked poses for each ligand were analysed by the PLP scoring system.

4.5. Biological assays

4.5.1. CtHtrA and HNE enzyme assays

Protocols for purification of the CtHtrA recombinant protein and biological assays were established in our previous publications [24, 26, 45, 46] and followed accordingly. In brief, six-dose series of **1** (0.01-125 µM) and equal volumes of DMSO were used to treat 2.5 µM of CtHtrA, using 10 µL of MeOCoum-ENLHLPLPIIF-DNP (Mimotopes) as the substrate. Proteolysis was monitored over 30 min at 37 °C, with multiple (3 x 3) readings taken every 30 s, each with 10 × flashes per well (340 nm excitation, 405 nm emission). All new compounds

at each dose were tested in triplicate, alongside **1** (n = 3) and DMSO control (n = 6). Non-linear regression analysis of the normalized response was performed in GraphPad Prism v 7.04.

The *in vitro* elastase (Athens Research and Technology) inhibition assay was performed by incubating elastase (final concentration, 186 nM) and inhibitor solution (final concentration, 0.12 μM to 31.25 μM) for 15 min at 37 °C before adding 100 μL of the substrate (methoxysuccinyl-Ala-Ala-Pro-Val-pNA; Sigma-Aldrich). All experiments were conducted in triplicate and the residual enzyme activity was measured by absorbance at 405 nm every 20 s for 10 min. IC_{50} values were derived by nonlinear regression of a normalized variable slope (four-parameter) model [26]. Enzyme activity was calculated in reference to the free enzyme (100% activity) and media controls (0% activity). Results are presented in the *Supporting Information*.

4.5.2. Chlamydia trachomatis and Chlamydia pecorum cell assays

C. trachomatis and *C. pecorum* cell culture assays were performed as reported in our previous papers [24, 48, 66]. In brief, *C. trachomatis* D (D/UW-3/Cx; CtD) and *C. pecorum* G (MC/MarsBar; CpG) were routinely cultured. Inhibition experiments were conducted with 96-well plates seeded with 20,000 host cells per well 24 h prior to the chlamydial infection. Infections were synchronised at 500 × g/28 °C for 30 min and cultures were treated with 25 μM, 50 μM and 100 μM doses of each compound at 16 h post-infection (PI) in triplicates, alongside 1% v/v DMSO and media-only controls. Cells were harvested 44 h PI, serially diluted onto fresh host cell monolayers, which were fixed and stained at 44 h PI for infectious yield quantification.

4.5.3. Cytotoxicity assessments against human epithelial monolayers

Cytotoxicity assays were carried out *as per* protocols established in Hwang *et al.* (2021) [26], which are outlined in 4.4.3.1 and 4.4.3.2.

4.5.3.1. MTS assay for cell metabolism and proliferation

MTS assays were performed using CellTiter 96® AQueous MTS Reagent Powder (Promega, Australia) following the manufacturer's instructions. HEp-2 cells were cultured (5000

cells/well) and treated with 1% v/v DMSO and inhibitors (25 µM and 100 µM doses), or media-only, 24 h post-culture. All treatments were performed in triplicate. At 24 h following treatment, the cells were incubated with MTS/phenazine methosulfate (PMS; Sigma) solution for 4 h, before measuring the absorbance at 490 nm.

4.5.3.2. LDH assay for cell integrity

Extracellular lactate dehydrogenase (LDH) was measured in treated HEp-2 cells by CytoTox 96® Non-Radioactive Cytotoxicity Assay (Promega, Australia), following the manufacturer's instructions. The cell density (5000 cells/well) matched that of the MTS assay. At 24 h post-culture, cells were treated with 25 µM and 100 µM of each **1** analogue, 1% v/v DMSO or media only. All experiments were performed in triplicates. After treatment for 8 h, supernatant was removed, treated with CytoTox reagent for 30 min, followed by the stop solution. Absorbance at 490 nm was measured. In addition, untreated cells were lysed with 0.8% v/v Triton X-100 to perform maximum release controls study 45 min prior to removal of the supernatant.

Acknowledgments

This project has been supported by the NSW Government under the NSW Koala Strategy. Jimin Hwang was supported by a University of Otago Doctoral Scholarship. Natalie Strange was supported by a UTS Faculty of Science HDR (Higher Degree by Research) Scholarship. The authors would like to thank the Department of Chemistry at the University of Otago for use of their NMR and mass spec facilities.

References

[1] L. Newman, J. Rowley, S. Vander Hoorn, N.S. Wijesooriya, M. Unemo, N. Low, G. Stevens, S. Gottlieb, J. Kiarie, M. Temmerman, Global Estimates of the Prevalence and Incidence of Four Curable Sexually Transmitted Infections in 2012 Based on Systematic Review and Global Reporting, PLoS One, 10 (2015) e0143304.
[2] C.L. Haggerty, S.L. Gottlieb, B.D. Taylor, N. Low, F. Xu, R.B. Ness, Risk of Sequelae after Chlamydia trachomatis Genital Infection in Women, J. Infect. Dis., 201 (2010) S134-S155.
[3] C.A. Leonard, N. Borel, Chronic Chlamydial Diseases: From Atherosclerosis to Urogenital Infections, Curr. Clin. Microbiol. Rep., 1 (2014) 61-72.
[4] S. Sethi, K. Zaman, N. Jain, Mycoplasma genitalium infections: current treatment options and resistance issues, Infect. Drug Resist., 10 (2017) 283-292.

[5] T.E. van der Schalk, J.F. Braam, J.G. Kusters, Molecular basis of antimicrobial resistance in Mycoplasma genitalium, Int. J. Antimicrob., 55 (2020) 105911-105911.
[6] A. Derbie, D. Mekonnen, Y. Woldeamanuel, T. Abebe, Azithromycin resistant gonococci: a literature review, Antimicrob. Resist. Infect. Control., 9 (2020) 1-138.
[7] K.M. Gernert, S. Seby, M.W. Schmerer, J.C. Thomas, C.D. Pham, S. St Cyr, K. Schlanger, H. Weinstock, W.M. Shafer, B.H. Raphael, E.N. Kersh, S. Hun, C. Hua, R. Ruiz, O.O. Soge, C. Dominguez, A. Patel, J. Loomis, J. Leavitt, J. Zhang, T. Baldwin, C. Wang, C. Moore, C. Whelen, P. O'Brien, A. Harvey, Azithromycin susceptibility of Neisseria gonorrhoeae in the USA in 2017: a genomic analysis of surveillance data, Lancet Microbe, 1 (2020) e154-e164.
[8] A.P.R.d. Costa-Lourenço, K.T. Barros dos Santos, B.M. Moreira, S.E.L. Fracalanzza, R.R. Bonelli, Antimicrobial resistance in Neisseria gonorrhoeae: history, molecular mechanisms and epidemiological aspects of an emerging global threat, Braz. J. Microbiol., 48 (2017) 617-628.
[9] C. McAlpine, D. Lunney, A. Melzer, P. Menkhorst, S. Phillips, D. Phalen, W. Ellis, W. Foley, G. Baxter, D. de Villiers, R. Kavanagh, C. Adams-Hosking, C. Todd, D. Whisson, R. Molsher, M. Walter, I. Lawler, R. Close, Conserving koalas: A review of the contrasting regional trends, outlooks and policy challenges, Biol. Conserv., 192 (2015) 226-236.
[10] M. TAYLOR/WWF-AUSTRALIA, Koala Extinction Risk NSW, in, 2018.
[11] D.o.A. Australian Government, Water and the Environment, *Phascolarctos cinereus* (combined populations of Qld, NSW and the ACT) — Koala (combined populations of Queensland, New South Wales and the Australian Capital Territory), in: Species Profile and Threats Database, 2021.
[12] R. Osawa, F.N. Carrick, Use of a dietary supplement in koalas during systemic antibiotic treatment of chlamydial infection, Aust. Vet. J., 67 (1990) 305-307.
[13] R.J. Melander, D.V. Zurawski, C. Melander, Narrow-spectrum antibacterial agents, MedChemComm, 9 (2018) 12-21.
[14] J. Skórko-Glonek, D. Figaj, U. Zarzecka, T. Przepiora, J. Renke, B. Lipinska, The extracellular bacterial HtrA proteins as potential therapeutic targets and vaccine candidates, Curr. Med. Chem, 24 (2017) 2174-2204.
[15] D.M. Roberts, Y. Personne, J. Ollinger, T. Parish, Proteases in Mycobacterium tuberculosis pathogenesis: potential as drug targets, Future Microbiol., 8 (2013) 621-631.
[16] W.E. Kaman, J.P. Hays, H.P. Endtz, F.J. Bikker, Bacterial proteases: targets for diagnostics and therapy, Eur. J. Clin. Microbiol. Infect. Dis., 33 (2014) 1081-1087.
[17] J. Sabotič, J. Kos, Microbial and fungal protease inhibitors—current and potential applications, Appl. Microbiol. Biotechnol., 93 (2012) 1351-1375.
[18] C. Moreno-Cinos, K. Goossens, I.G. Salado, P. Van Der Veken, H. De Winter, K. Augustyns, ClpP Protease, a Promising Antimicrobial Target, Int. J. Mol. Sci., 20 (2019) 2232.
[19] S. Backert, S. Bernegger, J. Skórko-Glonek, S. Wessler, Extracellular HtrA serine proteases: An emerging new strategy in bacterial pathogenesis, Cell. Microbiol., 20 (2018) e12845-n/a.
[20] S. Wessler, G. Schneider, S. Backert, Bacterial serine protease HtrA as a promising new target for antimicrobial therapy?, Cell Commun. Signal., 15 (2017) 4.
[21] R.-Y. Xue, C. Liu, Q.-T. Xiao, S. Sun, Q.-M. Zou, H.-B. Li, HtrA family proteases of bacterial pathogens: pros and cons for their therapeutic use, Clin. Microbiol. Infect., 27 (2020) 559-564.
[22] T. Clausen, M. Kaiser, R. Huber, M. Ehrmann, HTRA proteases: regulated proteolysis in protein quality control, Nat. Rev. Mol. Cell Biol., 12 (2011) 152.
[23] Z. Zhang, Q. Huang, X. Tao, G. Song, P. Zheng, H. Li, H. Sun, W. Xia, The unique trimeric assembly of the virulence factor HtrA from occurs via N-terminal domain swapping, J. Biol. Chem., 294 (2019) 7990.
[24] S. Gloeckl, V.A. Ong, P. Patel, J.D.A. Tyndall, P. Timms, K.W. Beagley, J.A. Allan, C.W. Armitage, L. Turnbull, C.B. Whitchurch, M. Merdanovic, M. Ehrmann, J.C. Powers, J. Oleksyszyn, M. Verdoes, M. Bogyo, W.M. Huston, Identification of a serine protease inhibitor which causes inclusion vacuole reduction and is lethal to *Chlamydia trachomatis*, Mol. Microbiol., 89 (2013) 676-689.
[25] A.A. Agbowuro, J. Hwang, E. Peel, R. Mazraani, A. Springwald, J.W. Marsh, L. McCaughey, A.B. Gamble, W.M. Huston, J.D.A. Tyndall, Structure-activity analysis of peptidic *Chlamydia* HtrA inhibitors, Bioorg. Med. Chem., 27 (2019) 4185-4199.
[26] J. Hwang, N. Strange, M.J.A. Phillips, A.L. Krause, A. Heywood, A.B. Gamble, W.M. Huston, J.D.A. Tyndall, Optimization of peptide-based inhibitors targeting the HtrA serine protease in

Chlamydia: design, synthesis and biological evaluation of pyridone-based and N-capping group-modified analogues, Eur. J. Med. Chem., 224 (2021) 113692-113692.
[27] M.A.T. Blaskovich, Unusual Amino Acids in Medicinal Chemistry, J. Med. Chem., 59 (2016) 10807-10836.
[28] A.K. Pandey, D. Naduthambi, K.M. Thomas, N.J. Zondlo, Proline Editing: A General and Practical Approach to the Synthesis of Functionally and Structurally Diverse Peptides. Analysis of Steric versus Stereoelectronic Effects of 4-Substituted Prolines on Conformation within Peptides, J. Am. Chem. Soc., 135 (2013) 4333-4363.
[29] N.Z. Alsharif, Medicinal chemistry and therapeutic relevance of angiotensin-converting enzyme inhibitors, Am. J. Pharm. Educ., 71 (2007) 123-123.
[30] A.A. Agbowuro, W.M. Huston, A.B. Gamble, J.D.A. Tyndall, Proteases and protease inhibitors in infectious diseases, Med. Res. Rev., (2017).
[31] I. Schechter, A. Berger, On the size of the active site in proteases. I. Papain, Biochem. Biophys. Res. Commun., 27 (1967) 157-162.
[32] B. Zhang, Comprehensive review on the anti-bacterial activity of 1,2,3-triazole hybrids, Eur. J. Med. Chem., 168 (2019) 357-372.
[33] M. Strzelecka, P. Świątek, 1,2,4-Triazoles as Important Antibacterial Agents, Pharmaceuticals (Basel), 14 (2021) 224.
[34] K. Bozorov, J. Zhao, H.A. Aisa, 1,2,3-Triazole-containing hybrids as leads in medicinal chemistry: A recent overview, Bioorg. Med. Chem., 27 (2019) 3511-3531.
[35] R. Gondru, S. Kanugala, S. Raj, C. Ganesh Kumar, M. Pasupuleti, J. Banothu, R. Bavantula, 1,2,3-triazole-thiazole hybrids: Synthesis, in vitro antimicrobial activity and antibiofilm studies, Bioorganic Med. Chem. Lett., 33 (2021) 127746.
[36] S. Zhang, Z. Xu, C. Gao, Q.-C. Ren, L. Chang, Z.-S. Lv, L.-S. Feng, Triazole derivatives and their anti-tubercular activity, Eur. J. Med. Chem., 138 (2017) 501-513.
[37] M. Kumari, S. Tahlan, B. Narasimhan, K. Ramasamy, S.M. Lim, S.A.A. Shah, V. Mani, S. Kakkar, Synthesis and biological evaluation of heterocyclic 1,2,4-triazole scaffolds as promising pharmacological agents, BMC Chem. Eng., 15 (2021) 5-5.
[38] N. Boechat, V.F. Ferreira, S.B. Ferreira, M.d.L.G. Ferreira, F.d.C. da Silva, M.M. Bastos, M.d.S. Costa, M.C.S. Lourenço, A.C. Pinto, A.U. Krettli, A.C. Aguiar, B.M. Teixeira, N.V. da Silva, P.R.C. Martins, F.A.F.M. Bezerra, A.L.S. Camilo, G.P. da Silva, C.C.P. Costa, Novel 1,2,3-Triazole Derivatives for Use against Mycobacterium tuberculosis H37Rv (ATCC 27294) Strain, J. Med. Chem., 54 (2011) 5988-5999.
[39] A. Rani, G. Singh, A. Singh, U. Maqbool, G. Kaur, J. Singh, CuAAC-ensembled 1,2,3-triazole-linked isosteres as pharmacophores in drug discovery: review, RSC Advances, (2020) 5610-5635.
[40] S.G. Agalave, S.R. Maujan, V.S. Pore, Click chemistry: 1,2,3-triazoles as pharmacophores, Chem. Asian J., 6 (2011) 2696-2718.
[41] A.A. Agbowuro, R. Mazraani, L.C. McCaughey, W.M. Huston, A.B. Gamble, J.D. Tyndall, Stereochemical basis for the anti-chlamydial activity of the phosphonate protease inhibitor JO146, Tetrahedron, (2017).
[42] D.K. Dalvie, A.S. Kalgutkar, S.C. Khojasteh-Bakht, R.S. Obach, J.P. O'Donnell, Biotransformation Reactions of Five-Membered Aromatic Heterocyclic Rings, Chem. Res. Toxicol., 15 (2002) 269-299.
[43] W.S. Horne, M.K. Yadav, C.D. Stout, M.R. Ghadiri, Heterocyclic Peptide Backbone Modifications in an α-Helical Coiled Coil, J. Am. Chem. Soc., 126 (2004) 15366-15367.
[44] S. Fletcher, The Mitsunobu Reaction in the 21st Century, ChemInform, 46 (2015) 739-752.
[45] W.M. Huston, J.D.A. Tyndall, W.B. Lott, S.H. Stansfield, P. Timms, Unique Residues Involved in Activation of the Multitasking Protease/Chaperone HtrA from Chlamydia trachomatis, PLoS One, 6 (2011) e24547.
[46] W.M. Huston, J.E. Swedberg, J.M. Harris, T.P. Walsh, S.A. Mathews, P. Timms, The temperature activated HtrA protease from pathogen Chlamydia trachomatis acts as both a chaperone and protease at 37°C, FEBS Lett., 581 (2007) 3382-3386.
[47] R. Wrase, H. Scott, R. Hilgenfeld, G. Hansen, The Legionella HtrA homologue DegQ is a self-compartmentizing protease that forms large 12-meric assemblies, Proc. Natl. Acad. Sci. U.S.A., 108 (2011) 10490.

[48] A. Lawrence, T. Fraser, A. Gillett, J.D.A. Tyndall, P. Timms, A. Polkinghorne, W.M. Huston, Chlamydia Serine Protease Inhibitor, targeting HtrA, as a New Treatment for Koala Chlamydia infection, Sci. Rep., 6 (2016) 31466.
[49] J. Lei, L. Sun, S. Huang, C. Zhu, P. Li, J. He, V. Mackey, D.H. Coy, Q. He, The antimicrobial peptides and their potential clinical applications, Am. J. Transl. Res., 11 (2019) 3919-3931.
[50] H.-G. Sahl, R.E.W. Hancock, Antimicrobial and host-defense peptides as new anti-infective therapeutic strategies, Nat. Biotechnol., 24 (2006) 1551-1557.
[51] M. Arik, A. Dorit, S. Yechiel, Ultrashort Antibacterial and Antifungal Lipopeptides, Proc. Natl. Acad. Sci. U.S.A., 103 (2006) 15997-16002.
[52] N.N. MohamedMohaideen, S.K. Palaninathan, P.M. Morin, B.J. Williams, M. Braunstein, S.E. Tichy, J. Locker, D.H. Russell, W.R. Jacobs, J.C. Sacchettini, Structure and Function of the Virulence-Associated High-Temperature Requirement A of Mycobacterium tuberculosis, Biochemistry, 47 (2008) 6092-6102.
[53] T. Krojer, J. Sawa, R. Huber, T. Clausen, HtrA proteases have a conserved activation mechanism that can be triggered by distinct molecular cues, Nat. Struct. Mol. Biol., 17 (2010) 844-852.
[54] S. Gloeckl, J.D.A. Tyndall, S.H. Stansfield, P. Timms, W.M. Huston, The Active Site Residue V266 of Chlamydial HtrA Is Critical for Substrate Binding during both in vitro and in vivo Conditions, J. Mol. Microbiol. Biotechnol., 22 (2012) 10-16.
[55] J.W. Marsh, W.B. Lott, J.D. Tyndall, W.W. Huston, Proteolytic activation of Chlamydia trachomatis HTRA is mediated by PDZ1 domain interactions with protease domain loops L3 and LC and beta strand beta5, Cell. Mol. Biol. Lett., 18 (2013) 522-537.
[56] E.S. Eberhardt, N. Panisik, R.T. Raines, Inductive Effects on the Energetics of Prolyl Peptide Bond Isomerization: Implications for Collagen Folding and Stability, J. Am. Chem. Soc., 118 (1996) 12261-12266.
[57] L.E. Bretscher, C.L. Jenkins, K.M. Taylor, M.L. Derider, R.T. Raines, Conformational stability of collagen relies on a stereoelectronic effect, J. Am. Chem. Soc., 123 (2001) 777-778.
[58] R.S. Erdmann, H. Wennemers, Conformational stability of collagen triple helices functionalized in the Yaa position by click chemistry, Org. Biomol. Chem., 10 (2012) 1982-1986.
[59] R. Gomez, R.M. Obella, D.A. Powell, Carbocyclic prolinamide derivatives. Patent WO201722914A1, in: W.I.P. Organization (Ed.), December 17, 2017.
[60] B.C. Boren, S. Narayan, L.K. Rasmussen, L. Zhang, H. Zhao, Z. Lin, G. Jia, V.V. Fokin, Ruthenium-Catalyzed Azide−Alkyne Cycloaddition: Scope and Mechanism, J. Am. Chem. Soc., 130 (2008) 8923-8930.
[61] C. The UniProt, UniProt: the universal protein knowledgebase in 2021, Nucleic Acids Res., 49 (2021) D480-D489.
[62] C. Notredame, D.G. Higgins, J. Heringa, T-Coffee: A Novel Method for Fast and Accurate Multiple Sequence Alignment, J. Mol. Biol., 302 (2000) 205-217.
[63] M.-y. Shen, A. Sali, Statistical potential for assessment and prediction of protein structures, Protein Sci., 15 (2006) 2507-2524.
[64] M.D. Hanwell, D.E. Curtis, D.C. Lonie, T. Vandermeersch, E. Zurek, G.R. Hutchison, Avogadro: an advanced semantic chemical editor, visualization, and analysis platform, J. Cheminformatics, 4 (2012) 17.
[65] C.A. Veale, P.R. Bernstein, C. Bryant, C. Ceccarelli, J.R. Damewood, Jr., R. Earley, S.W. Feeney, B. Gomes, B.J. Kosmider, Nonpeptidic inhibitors of human leukocyte elastase. 5. Design, synthesis, and x-ray crystallography of a series of orally active 5-aminopyrimidin-6-one-containing trifluoromethyl ketones, J. Med. Chem., 38 (1995) 98-108.
[66] J.S. Hocking, L.A. Vodstrcil, W.M. Huston, P. Timms, M.Y. Chen, K. Worthington, R. McIver, S.N. Tabrizi, i. Australian Chlamydia Treatment Study, A cohort study of Chlamydia trachomatis treatment failure in women: a study protocol, BMC Infect. Dis., 13 (2013) 379-379.